

1 Urea based Foldamers

2 Sung Hyun Yoo, Bo Li, Christel Dolain, Morgane Pasco, Gilles Guichard

3 Univ. Bordeaux, CNRS, Bordeaux INP, CBMN, UMR 5248, Institut Européen de Chimie et Biologie, 2 rue

4 Robert Escarpit, F-33607, Pessac, France

5

6 ABSTRACT

7 *N,N'*-linked oligoureas are a class of enantiopure, sequence-defined peptidomimetic oligomers
8 without amino acids that form well-defined and predictable helical structures akin to the peptide α -
9 helix. Oligourea based foldamers combine a number of features – such as synthetic accessibility,
10 sequence modularity, and folding fidelity – that bode well for their use in a range of applications from
11 medicinal chemistry to catalysis. Moreover, it was recently recognized that this synthetic helical
12 backbone can be combined with regular peptides to generate helically folded peptide-oligourea
13 hybrids that display additional features in terms of helix mimicry and protein-surface recognition
14 properties. Here we provide detailed protocols for the preparation of requested monomers and for
15 the synthesis and purification of homo oligoureas and peptide-oligourea hybrids.

16

17 CONTENTS

18 1. Introduction

19 2. Helical structures of *N,N'*-linked oligoureas and oligourea/peptide chimeras

20 3. Applications of urea-based foldamers

21 3.1 Cationic amphiphilic foldamers as host-defense peptide mimics and for the delivery of
22 nucleic acids

23 3.2 Nanostructures by self-assembly of amphiphilic water soluble oligoureas

24 3.3 Chimeric helices as inhibitors of protein-protein interactions and as receptor ligands

25	3.4	Composite proteins containing foldamer segments
26	3.5	Anion recognition, organocatalysis and electron transfer
27	4.	Main strategies to synthesize oligourea based foldamers
28	4.1	Synthesis of oligoureas in solution
29	4.2	Fragment condensation
30	4.3	Solid phase synthesis of oligoureas
31	5.	Synthetic protocols
32	5.1	Materials
33	5.1.1	Reagents
34	5.1.2	Equipment
35	5.2	Monomer preparation
36	5.2.1	Azide type monomers bearing the side chain at the β C position (N_3 -Xaa ^{β} -OSu)
37	5.2.2	Azide type monomers bearing the side chain at the α C position (N_3 -Xaa ^{α} -OSu)
38	5.3	Synthesis of oligourea based foldamers on solid support
39	5.3.1	Solid phase synthesis of oligoureas
40	5.3.2	Solid phase synthesis of hybrid peptide-oligourea (PUH) or oligourea-peptide
41		(UPH) sequences
42	5.3.3	Purification and characterization of oligourea-based foldamers
43	5.3.4	Troubleshooting
44	6.	Concluding remarks and future directions

45

46 **KEYWORDS**

47 Foldamers, Oligourea, Peptide mimicry, Helix, Protein surface recognition, Protein-protein
48 interactions, Chimeric peptide/oligourea helices, Solid-phase synthesis

49

50 1. INTRODUCTION

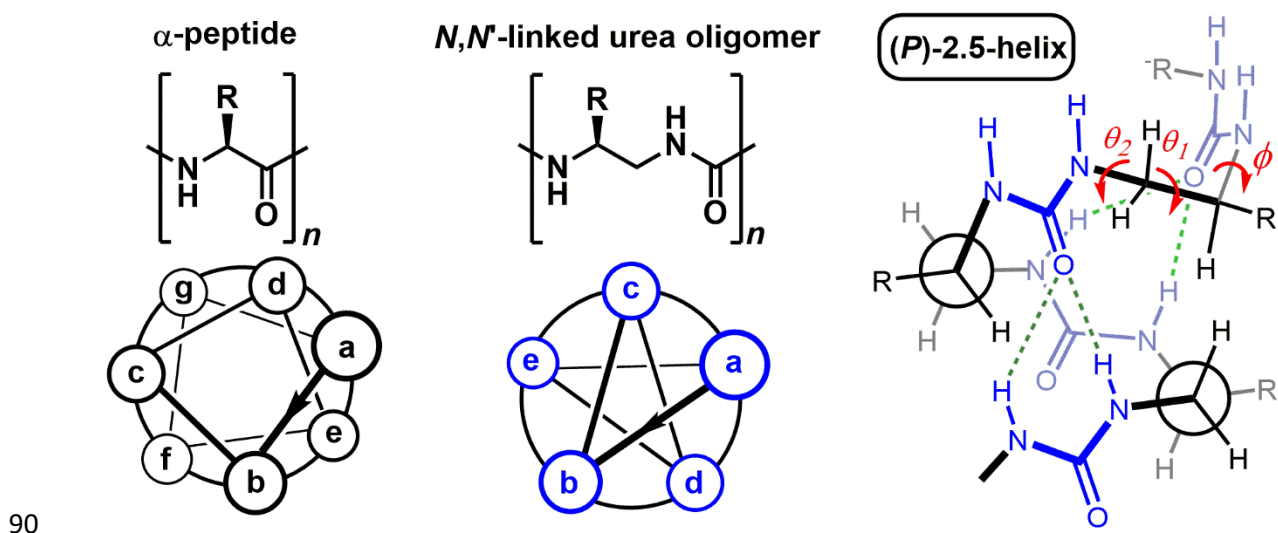
51 Advances in foldamer research have led to the discovery of a wide range of non-natural synthetic
52 oligomers predisposed to adopt well-defined folded structures akin to those found in proteins and
53 nucleic acids(Gellman, 1998; Goodman, Choi, Shandler, & DeGrado, 2007; Gilles Guichard & Huc, 2011;
54 Horne & Grossmann, 2020; Johnson & Gellman, 2013; Seebach, Beck, & Bierbaum, 2004). These
55 synthetic sequence-specific backbones inspired by biopolymers obey different folding and self-
56 assembly rules and provide enticing opportunities to explore entirely new chemical spaces. Although
57 the creation of synthetic folded architectures was initially largely driven by curiosity, with a focus on
58 exploration and conformational analysis of new backbones, it quickly turned out that the ability to
59 synthesize sequence-based oligomers that fold with high fidelity raised the possibility of creating
60 molecules with defined functions. In particular, it has been shown that biopolymer mimicry with
61 foldamers can provide unique tools to study biology and may lead to the elaboration of novel
62 diagnostic/therapeutic agents (Azzarito, Long, Murphy, & Wilson, 2013; Checco & Gellman, 2016;
63 Gopalakrishnan, Frolov, Knerr, Drury, & Valeur, 2016; Johnson & Gellman, 2013; Pasco, Dolain, &
64 Guichard, 2017). For example, α/β -peptides which are faithful α -helix mimics have been developed as
65 inhibitors of protein-protein interactions or as receptor ligands with improved pharmacological
66 properties, increased resistance to proteolytic degradation and in some cases prolonged duration of
67 action in vivo(Boersma et al., 2011; Checco et al., 2015; Cheloha, Maeda, Dean, Gardella, & Gellman,
68 2014; Horne et al., 2009; Johnson et al., 2014; Johnson & Gellman, 2013; Kritzer, Hodsdon, &
69 Schepartz, 2005; Kritzer, Stephens, Guarracino, Reznik, & Schepartz, 2005; Lee et al., 2009; Liu,
70 Cheloha, Watanabe, Gardella, & Gellman, 2018; Liu et al., 2019; Michel, Harker, Tirado-Rives,
71 Jorgensen, & Schepartz, 2009). Furthermore, the ability to link sequence and folding within non-
72 biological synthetic foldamers can be exploited to create architectures reaching the size and
73 complexity of small proteins (tertiary and quaternary structures) (Horne & Grossmann, 2020; Pappas
74 et al., 2020) or molecular strands that display molecular recognition properties and functions beyond
75 those found in nature(Ferrand & Huc, 2018; Gan et al., 2017).

86 Besides aliphatic and aromatic oligoamide foldamers which have been extensively studied, a few other
 87 backbones that do not contain an amide linkage and show high folding propensity have emerged as
 88 potentially useful proteinomimetics. This is the case of aliphatic N,N' -linked urea oligomers (Burgess,
 89 Shin, & Linthicum, 1995) which were found to form surprisingly well-defined and stable helical
 90 secondary structures reminiscent of the α -helix (Lucile Fischer et al., 2010; Lucile Fischer & Guichard,
 91 2010; Semetey, Rognan, et al., 2002). Chiral oligoureia foldamers combine a number of unique and
 92 positive features – such as synthetic accessibility, sequence modularity, and high folding fidelity – that
 93 bode well for their use in a range of applications from medicinal chemistry to catalysis.

84

85 2. HELICAL STRUCTURES OF N,N' -LINKED OLIGOUREAS AND OLIGOUREA/PEPTIDE CHIMERAS

86 In solution and in the crystal, enantiopure aliphatic N,N' -linked oligoureias adopt a helical fold, termed
 87 a 2.5-helix, with 2.5 residues per helical turn and a pitch of 5.1 Å stabilized by intramolecular three-
 88 centered H-bonds closing 12- and 14-membered H-bonded pseudorings (Fig. 1) (G. W. Collie, K. Pulka-
 89 Ziach, & G. Guichard, 2016; Lucile Fischer et al., 2010; A. Violette et al., 2005).

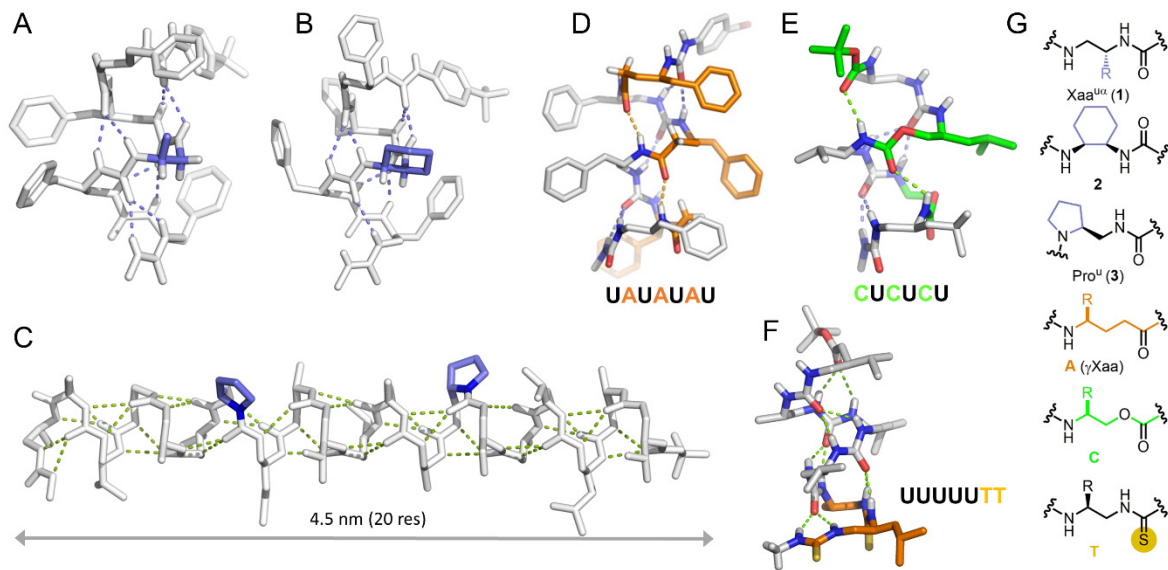


91 **Fig. 1.** Comparison of α -peptide $(Xaa)_n$ and N,N' -linked oligoureia $(Xaa^u)_n$ backbones and representation
 92 of the 2.5-helical conformation of oligoureias showing the three center H-bond network. Ureido
 93 residues are denoted Xaa^u (X^u) by analogy to the three (one) letter code of α -amino acids

94

95 The helicity of urea oligomers is largely unaffected by the nature of the side chains in the sequence (in
96 contrast to α -peptides), which makes these foldamers robust and tunable, allowing the different side
97 chains (including polar ones) to be faithfully displayed at the helix surface. The chemical accessibility
98 of the chiral ethylene diamine based monomers permits the synthesis of urea oligomers that bear, yet
99 are not limited to, any of the 20 naturally occurring amino-acid side chains. Over the years, we and
100 others have continuously expanded the repertoire of monomers(Douat-Casassus, Pulka, Claudon, &
101 Guichard, 2012; Legrand et al., 2012; Y.-R. Nelli et al., 2012; Pendem, Douat, et al., 2013; Wechsel,
102 Raftery, Cavagnat, Guichard, & Clayden, 2016) and improved oligomer synthesis by generalizing
103 solution(Fremaux, Fischer, Arbogast, Kauffmann, & Guichard, 2011) and solid-phase methods(Burgess
104 et al., 1995; Douat-Casassus et al., 2012; Gilles Guichard, Semetey, Rodriguez, & Briand, 2000; Kim, Bi,
105 Paikoff, & Schultz, 1996) (see **section 4** “Main strategies to synthesize oligoureia based foldamers”).

106 Thorough exploration of the requirements for secondary structure formation has shown how variation
107 of substitution patterns (*e.g.* *N*-pyrrolidine units (proline analogue)(Fremaux et al., 2011; Fremaux,
108 Kauffmann, & Guichard, 2014), constrained *cis*-cyclohexyl diamine units(Pendem, Nelli, et al., 2013;
109 Wechsel et al., 2016) and even bulkier 1,2-diaminobicyclo[2.2.2]octane bicyclic units(Legrand et al.,
110 2012; Milbeo et al., 2020)), shifted side chain from β C to α C with inversion of stereochemistry; Fig. 2A-
111 C)(Pendem, Nelli, et al., 2013) and isosteric backbone modifications (*e.g.* insertion of γ -amino acid
112 residues, carbamate or thiourea linkages; Fig. 2D-G)(Y. R. Nelli et al., 2015; Y. R. Nelli, Fischer, Collie,
113 Kauffmann, & Guichard, 2013; Pendem, Nelli, et al., 2013) can be used to modulate helix properties
114 and generate different spacing and orientation of side chains at the surface.



115

116 **Fig. 2.** Crystal structures of a pentapeptide with a (A) shifted substitution pattern and a (B) constrained
 117 cyclohexyl ring at central residue;(Pendem, Douat, et al., 2013), (C) crystal structure of a 20-mer
 118 oligoureia with two pyrrolidine units forming a long (45 Å) helical segment;(Fremaux et al., 2011);
 119 crystal structures of heterogeneous backbones consisting of (D) alternating urea/amide units, (E)
 120 alternating urea/carbamate units(Pendem, Nelli, et al., 2013) and (F) mixed urea/thiourea linkages.(Y.
 121 R. Nelli et al., 2015); (G) Example of monomers with non-canonical substitution patterns (Xaa^{uα}(1) *cis*-
 122 cyclohexyl (2), Pro^u (3) and urea isosteric units (γ-amino acid (γXaa) A, carbamate C and thiourea T
 123 linkages) compatible with helix formation.

124

125 The similarities in screw sense, pitch and polarity between peptide α-helices and oligoureia 2.5-helices
 126 also suggested to us that these two backbones could be combined, thus permitting key beneficial
 127 features of both species—such as natural epitope recognition of α-peptides and the innate helical
 128 stability of oligoureias—to be exploited in single chimeric constructs. We first investigated model
 129 chimeric α-peptide/oligoureia and oligoureia/α-peptide sequences to define the rules that govern helix
 130 formation in these sequences. The resulting chimeras (*i.e.* “block cofoldamers”) with aliphatic
 131 oligoureias fused to short peptide segments (either at the N- or C-terminus or at both termini) were
 132 found to adopt a continuous helical structure in the solid state as well as in polar organic solvents, the
 133 peptide and oligoureia helices being connected by a unique H-bond network(Fremaux et al., 2015;
 134 Mauran, Kauffmann, Odaert, & Guichard, 2016). The finding that oligoureia foldamers can be interfaced
 135 with natural peptide helices and that the two helical forms do communicate within a single strand is

136 of particular significance for applications of foldamers in biology. Possible benefits of generating such
137 chimeric helices include improved nucleation of α -helical peptide segments, increased resistance to
138 proteolysis and prolonged activities *in vivo*.

139

140 **3. APPLICATIONS OF UREA-BASED FOLDAMERS**

141 The ability to synthesize diverse, sequence-specific oligoureas that fold with a high degree of
142 predictability has stimulated the interest of our group and others to endow urea-based foldamers with
143 function. Examples of applications reported for urea-based foldamers range from bioactive peptide
144 mimics(Fremaux, Venin, Mauran, Zimmer, Guichard, et al., 2019) including modulators of protein-
145 protein interactions(Cussol et al., 2021) to quaternary structures(Collie et al., 2015) and from electron
146 transfer(Pulka-Ziach & Sęk, 2017) to catalysis(Bécart et al., 2017). Some of these applications are
147 discussed in more detail below.

148 **3.1 Cationic amphiphilic foldamers as host-defense peptide mimics and for the delivery of nucleic** 149 **acids**

150 Short chain oligoureas designed to mimic globally amphiphilic cationic α -helical host-defense peptides
151 have been found to be active against a range of Gram-negative and Gram-positive bacteria(Claudon et
152 al., 2010; Aude Violette et al., 2006). These oligoureas which display a high helical content in the vicinity
153 of phospholipid membranes are thought to be active by a mechanism involving permeabilization of
154 the bacterial membrane. One such foldamer was found to be active against bacterial forms of *Bacillus*
155 *anthracis* encountered *in vivo* (*i.e.*, germinating spores, encapsulated and non-encapsulated bacilli)
156 and to exert partial protection in cutaneous and inhalational models of infection with *B.*
157 *anthracis*(Teyssières et al., 2016).

158 Sequence variations such as pH-responsive side chains and dimerization were introduced to convert
159 these antimicrobial foldamers into gene transfection agents. Bioreducible helical cell penetrating
160 foldamers (CPFs) with high capacity to assemble with plasmid DNA and to deliver nucleic acids into the

161 cell were finally obtained by thiol-mediated dimerization of a short (8-mer) amphipathic helical
162 oligourea bearing His and Arg side chains. The best compound in this series was found to compare
163 favorably in terms of transfection efficiency with LAH4, a His-rich peptide CPP with high transfection
164 ability(Douat et al., 2015). New CPF sequences with activity in culture medium containing up to 50%
165 of serum as well as sequences for siRNA delivery were reported recently(Bornerie, Brion, Guichard,
166 Kichler, & Douat, 2021; Douat, Bornerie, Antunes, Guichard, & Kichler, 2019).

167 **3.2 Nanostructures by self-assembly of amphiphilic water soluble oligoureas**

168 A recent extension of this early work is the design of amphiphilic water-soluble foldamer sequences
169 for the precise construction of nanometer scale assemblies mimicking protein quaternary
170 structures(Gavin William Collie, Karolina Pulka-Ziach, & Gilles Guichard, 2016; Collie et al., 2015;
171 Caterina M. Lombardo et al., 2016; Yoo, Collie, Mauran, & Guichard, 2020). We have shown that it is
172 possible to orient the assembly process towards compact (bundles) or extended nanostructures
173 (fibrils, nanotubes) in aqueous conditions by sequence manipulation and redistribution of charged side
174 chains (Fig. 3B). Importantly, we found that compact nanostructures obtained by the assembly of
175 designed amphiphilic oligourea helices possess isolated internal cavities large enough to host guest
176 molecules(Collie et al., 2017).

177 **3.3 Chimeric helices as inhibitors of protein-protein interactions and as receptor ligands**

178 The structural similarity between oligourea and peptide helices suggests that the introduction of
179 oligourea inserts into bioactive peptides could be used to generate effective inhibitors of protein-
180 protein interactions or receptor ligands with a reduced peptide character (Fig. 3C). However, one
181 difficulty associated with the use of foldamers as α -helix mimics is to select and arrange key side chains
182 on the surface of the foldamer so as to maintain key contacts with the target. By selecting ubiquitin
183 ligase MDM2, vitamin D receptor and histone chaperon ASF1 as targets, we have designed
184 peptide/oligourea chimeras that retain affinity for their protein target while showing increased
185 resistance to proteolysis(Cussol et al., 2021; Mbianda et al., 2020). X-ray structure analysis of several

186 of these peptide–oligourea hybrids bound to their respective protein targets confirms the high degree
187 of α -helix mimicry that can be achieved with oligoureas and reveals general principles that should
188 enable the design of more potent peptide-based inhibitors of protein–protein interactions.

189 Peptide-oligourea chimeras have also been used to generate mimics of Class-B GPCR ligands with
190 increased resistance to proteolytic degradation. In particular, we have shown that oligourea foldamers
191 are effective tools to improve the pharmaceutical properties of GLP-1, a 31-amino acid peptide
192 hormone involved in metabolism and glycemic control. Our strategy consisted in replacing four
193 consecutive amino acids of GLP-1 by three consecutive ureido residues by capitalizing on the structural
194 resemblance of oligourea and α -peptide helices. The efficacy of the approach was demonstrated with
195 three GLP-1-oligourea hybrids showing prolonged activity *in vivo* (Fremaux, Venin, Mauran, Zimmer,
196 Guichard, et al., 2019). We have also shown that modified GLP-1 analogues with a single ureido residue
197 replacement at position 2 exhibit antidiabetic properties and longer duration of action via selective
198 enhancement of G protein-dependent cAMP signaling and altered GLP-1R trafficking (Fremaux, Venin,
199 Mauran, Zimmer, Koensgen, et al., 2019).

200 **3.4 Composite proteins containing foldamer segments**

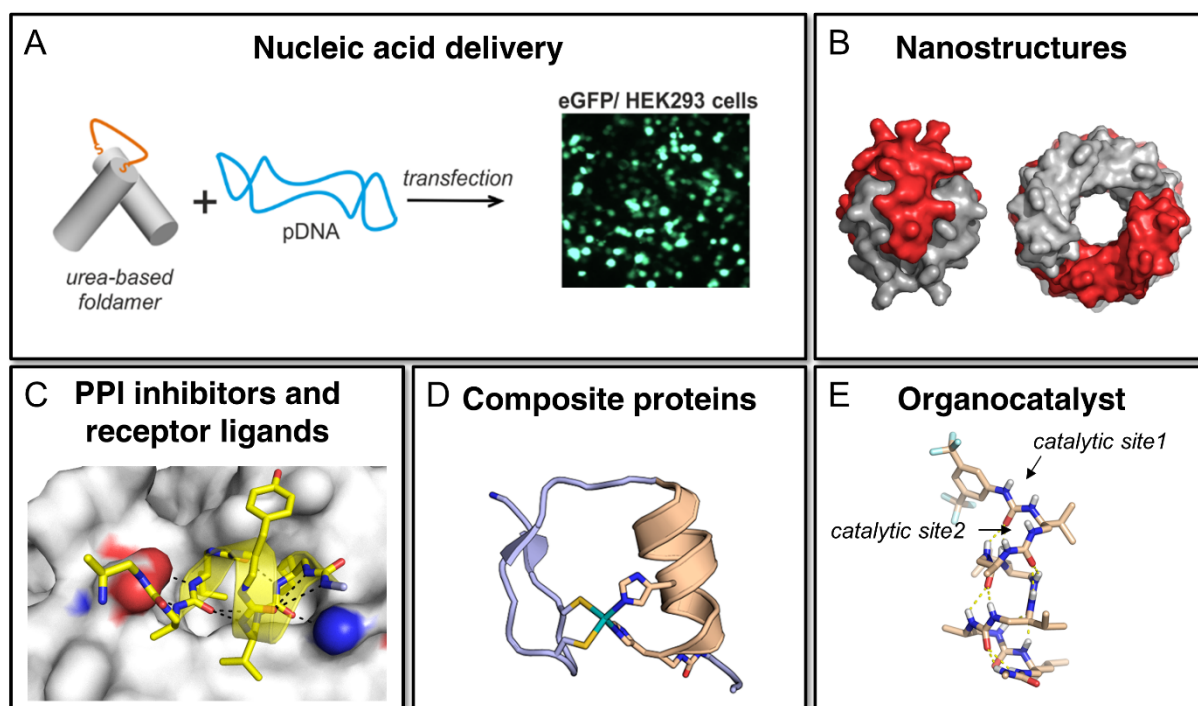
201 Encouraged by the similarity between peptide and oligourea helices, we have explored the chemical
202 synthesis, folding, and function of composite proteins created by substituting one α -helical regions of
203 a target protein by non-peptide helical segments (urea-based foldamers; Fig. 3D). Such composite
204 proteins may prove useful to interrogate protein folding, address the role of individual folded segments
205 and modulate protein function and properties. We moved a step towards the creation of such
206 composite proteins by replacing the 10-residue long original α -helical segment in the Cys2His2 zinc
207 finger 3 of transcription factor Egr1 (also known as Zif268) by an oligourea sequence bearing two
208 appropriately spaced imidazole side chains for zinc coordination (C. M. Lombardo et al., 2019).
209 Cys2His2 zinc fingers are recurrent protein motifs involved in specific duplex DNA recognition of about
210 30 residues, which consist of two antiparallel strands of β -sheet connected by a turn, packed against

211 an α -helix(Wolfe, Nekludova, & Pabo, 2000). This archetypal $\beta\beta\alpha$ fold is stabilized by a single zinc ion
212 coordinated by a pair of cysteine residues located in the β -sheet and a pair of histidine residues located
213 at the C-terminus of the α -helix in a tetrahedral geometry. We have shown by spectroscopic
214 techniques and mass spectrometry analysis under native conditions that the ability of the
215 peptide/oligourea hybrid to coordinate zinc ion was not affected by the introduction of the foldamer
216 insert. Moreover, detailed NMR analysis provided evidence that the engineered zinc finger motif
217 adopts a folded structure in which the native β -sheet arrangement of the peptide region and global
218 arrangement of DNA binding side chains are preserved. Titration in the presence of Egr1 target DNA
219 sequence also supported binding to GC bases as reported for the wild type motif.

220 **3.5 Anion recognition, organocatalysis and electron transfer**

221 Oligoureas typically mediate interactions through their side chains but the main chain ureas also
222 display interesting molecular recognition properties. We have shown that the helical oligourea
223 backbone is well preorganized to bind small guest molecules such as anions. ^1H NMR studies in various
224 organic solvents including DMSO revealed that anions such as carboxylate bind at the positive end of
225 the helix macrodipole without causing helix unfolding(Diemer, Fischer, Kauffmann, & Guichard, 2016).
226 This property was exploited to induce screw-sense preference of achiral oligourea helices consisting
227 of meso-cyclohexane-1,2-diamine monomers by selective formation of a 1:1 hydrogen-bonded
228 complex with a chiral carboxylate anion(Wechsel et al., 2016; Wechsel, Žabka, Ward, & Clayden, 2018).
229 Taking inspiration from these studies, we envisioned that helical oligo(thio)urea foldamers could be
230 designed to catalyze enantioselective C-C bond formation. The catalytic system we designed is
231 composed of two modules, including an oligourea hexamer as the H-bonding chiral component (Fig.
232 3E) and a tertiary amine as a base component. We have shown that this system promotes the Michael
233 reaction between enolizable carbonyl compounds and nitroolefins at remarkably low chiral catalyst
234 loading with high enantioselectivity(Bécart et al., 2017). Structure-activity relationship studies
235 revealed a strong correlation between the oligomer catalyst efficiency and its folding propensity. This

236 catalytic system can be readily optimized, as each component can be separately fine-tuned to increase
237 reaction rates, selectivity, and other properties.



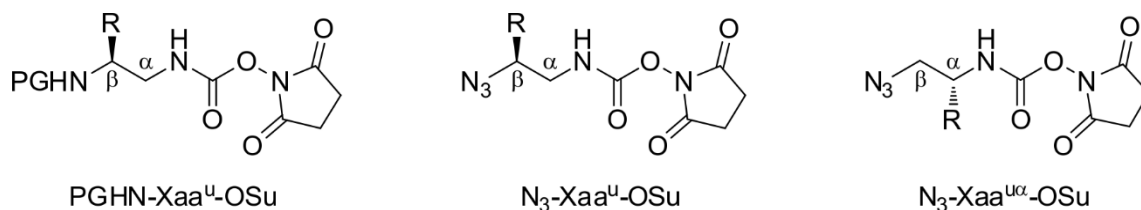
238

239 **Fig. 3.** Some Applications of urea-based foldamers. (A) pH-responsive dimeric urea-based foldamers to
240 enhance cellular uptake of nucleic acids. (B) X-ray structures of a hexameric bundle (left) and a helical
241 nanotube (right) formed by self-assembly of designed amphiphilic oligourea helices. (C) X-ray structure
242 of a short oligourea helix (yellow) mimicking key residues of the steroid receptor coactivator SRC2-3 in
243 complex with the vitamin D receptor. (D) NMR-derived low energy structure of a composite zinc finger
244 containing a nonpeptide foldamer helical domain (peptide in light blue and oligourea in salmon). (E)
245 Atomic structure of a hydrogen bonding oligourea-based chiral catalyst. *Sources* : (A) Reprinted with
246 permission from . Copyright 2015 John Wiley & Sons Inc. (B) : Reprinted with permission from .
247 Copyright 2015 Springer Nature. (C) Reprinted with permission from . Copyright 2021 John Wiley &
248 Sons Inc. (D) Reprinted with permission from . Copyright 2019 American Chemical Society. (E)
249 Reprinted with permission from . Copyright 2017 American Chemical Society.
250

251 4. MAIN STRATEGIES TO SYNTHESIZE OLIGOUREA BASED FOLDAMERS

252 Both solution and solid phase methods have been developed to synthesize enantiopure aliphatic *N,N'*-
253 linked oligoureas. They are based on a sequential coupling of monoprotected chiral 1,2-diamine
254 monomers activated as *O*-succinimidyl carbamates. With six positions for substituents (compare **1**, **2**
255 and **3** in Fig. 2), these building blocks are incredibly diverse (for comparison α -amino acids contain
256 three positions for substituents whereas β -amino acids have five). Monomers substituted at either the

257 α C or the β C position can be conveniently prepared in a few steps from α -amino acids bearing any of
258 the 20 naturally occurring amino-acid side chains (Fig. 4).



260 **Fig. 4.** Chemical structures of monoprotected chiral 1,2-diamine monomer and azide-type monomers,
261 activated as *O*-succinimidyl carbamates. Ureido residues are denoted Xaa^u by analogy to the three-
262 letter code of α -amino acids, and Xaa^{u α} related to shifted side chain from β C to α C.

263

264 4.1 Synthesis of oligoureas in solution

265 The synthesis of short oligourea sequences can be efficiently performed in solution using Boc-
266 protected monomers by iterative coupling and deprotection steps (G. Guichard et al., 1999). The
267 reaction of the activated carbamate with a primary or secondary amine proceeds rapidly in presence
268 of *Hünig's* base at room temperature, and the only by-product formed – *i.e.* *N*-hydroxysuccinimide, is
269 easily removed by aqueous workup. A short purification by flash chromatography or recrystallization
270 affords the pure ureido derivative in good yields. The Boc-deprotection step is performed in the
271 presence of TFA at 0°C, and the resulting trifluoroacetate salt which is frequently recovered after Et₂O
272 precipitation is used without further purification. Oligomers bearing up to 9 urea residues were
273 obtained in high yields and in a sequence controlled manner using this synthesis route. However, to
274 overcome solubility issues, and increase the efficacy of synthesis in the case of longer and diverse
275 oligourea sequences, other strategies, such as convergent fragment condensation or stepwise solid-
276 phase synthesis techniques were developed.

277 4.2 Fragment condensation

278 Convergent coupling is a useful alternative to stepwise synthesis – whose efficacy starts to decrease
279 beyond 10 residues due to solubility and/or purification issues – for accessing longer oligomers.
280 Fragment condensation requires an oligourea segment to be activated as a succinimidyl carbamate at

281 one end, prior to coupling to the terminal amine of a second oligourea segment. However, the
282 activation of oligoureas is impaired by the formation of a cyclic biuret resulting from the attack of the
283 formed succinimidyl carbamate by the nearest urea NH (Fremaux et al., 2011; Semetey, Didierjean,
284 Briand, Aubry, & Guichard, 2002). The introduction of a protecting group on this specific NH or the use
285 of a *N*-alkylated terminal residue instead (*e.g.* a proline derived monomer) circumvented this synthetic
286 issue allowing activated oligoureas to be readily prepared. The fragment condensation step was found
287 to proceed in good to high yield when using a pyrrolidine ring at the segment junction and long helical
288 oligoureas up to 20 residues were obtained by iterative segment couplings(Fremaux et al., 2011).

289 **4.3 Solid phase synthesis of oligoureas**

290 We initially used Fmoc-protected monomers and standard protocols adapted from solid-phase peptide
291 synthesis (SPPS) to prepare oligoureas on solid support(Gilles Guichard et al., 2000). Although short
292 (up to seven residues) oligourea sequences were obtained in good yields and purities, the coupling
293 steps required long reaction times (several hours) and a large excess of monomers (at least double
294 couplings with 3 equiv. of monomers). Next, we thought to employ microwave irradiation, a
295 widespread technique in SPPS to increase coupling rates and accelerate synthesis. However, we found
296 that the Fmoc-protected monomers activated as *O*-succinimidyl carbamates were not compatible with
297 microwave irradiation leading to uncontrolled oligomerization on resin. The SPS of oligoureas using
298 Boc-protected monomers and microwave assistance proved to be a much more robust strategy.
299 Because the urea linkage formed by anchoring the first residue on MBHA-type resins was found to be
300 sensitive to the acidic conditions required to cleave the Boc group, we introduced an isosteric γ^4 -amino
301 acid as the first residue to enable the formation of a stable amide bond onto the resin, prior to
302 elongation of the oligourea sequence (Claudon et al., 2010). Excellent results in terms of synthesis
303 efficiency (excess of monomers was substantially reduced and speed of synthesis was increased), and
304 purity of crude products have been obtained. Yet the final HF cleavage from the resin renders this
305 strategy not practical for routine syntheses in the laboratory.

306 To combine both the convenient use of standard TFA-labile resins and the efficiency of microwave-
307 assisted coupling steps, we finally turned to monomers bearing azide as a masked amine for the SPS
308 of oligoureas (Douat-Casassus et al., 2012). Thus far, the best conditions identified for on-resin
309 reduction of azido-terminated oligoureas involve the use of trimethylphosphine with microwave
310 assistance. This method is compatible with automation and parallel synthesis and is now routinely used
311 in our laboratory to prepare oligoureas and related peptide-oligourea hybrids (Antunes, Douat, &
312 Guichard, 2016; Cussol et al., 2021). The detailed synthetic procedures are reported in **section 5.3**.

313 **5. SYNTHETIC PROTOCOLS**

314 **5.1 Materials**

315 **5.1.1 Reagents**

316 *5.1.1.1 Chemicals*

317 Fmoc α -amino acids

318 Isobutyl chloroformate (IBCF)

319 *N*-Methylmorpholine (NMM)

320 Sodium borohydride (NaBH₄)

321 1,8-diazabicyclo[5.4.0]undec-7-ene (DBU)

322 Trifluoroacetic acid (TFA)

323 Triphenylphosphine (PPh₃)

324 Phthalimide

325 Diisopropyl azodicarboxylate (DIAD)

326 Methanesulfonyl chloride (MsCl)

327 *N,N'*-disuccinimidyl carbonate (DSC)

- 328 Imidazole-1-sulfonyl azide hydrochloride ($\text{N}_3\text{SO}_2\text{Im}\cdot\text{HCl}$) (prepared as described in literature(Goddard-
- 329 Borger & Stick, 2007, 2011)
- 330 Copper (II) sulfate pentahydrate ($\text{CuSO}_4\cdot 5\text{H}_2\text{O}$)
- 331 Triethylamine (Et_3N)
- 332 Sodium azide (NaN_3)
- 333 Iodine (I_2)
- 334 Imidazole
- 335 Sodium chloride (NaCl)
- 336 Sodium bicarbonate (NaHCO_3)
- 337 Potassium carbonate (K_2CO_3)
- 338 Potassium hydrogen sulfate (KHSO_4)
- 339 Magnesium sulfate (MgSO_4)
- 340 *N,N*-diisopropylethylamine (DIEA)
- 341 Isopropyl isocyanate
- 342 Triisopropylsilane (TIS)
- 343 Piperidine
- 344 *N,N'*-diisopropylcarbodiimide (DIC)
- 345 Ethyl-2-cyano-2-(hydroxyimino)acetate (Oxyma)
- 346 Trimethylphosphine solution (1M in tetrahydrofuran).
- 347 *5.1.1.2 Resins*
- 348 Rink Amide MBHA resin (Novabiochem #8550030005, loading of 0.52 mmol/g).

349 5.1.1.3 Solvents

350 Dry DCM and THF are obtained by filtration through activated alumina using a dedicated purification
351 system (MBRAUN SPS-800) and should be used immediately. The other solvents are purchased from
352 commercial sources and used without any further purification. Specific solvent grades are
353 recommended for the solid phase synthesis: *N,N*-dimethylformamide (DMF, Carlo Erba #P0343521, for
354 peptide synthesis), dichloromethane (DCM, Carlo Erba #412622000, HPLC grade), 1,4-dioxane (Carlo
355 Erba #338003) and acetonitrile (MeCN, Carlo Erba #412409, HPLC grade), water (mQ grade).

356 5.1.2 Equipment

357 Magnetic stirrer with temperature sensor (Heidolph), Balance (Mettler Toledo), UV lamp (Vilber),
358 Rotary evaporator (Buchi or Heidolph), Bath sonicator (Bioblock Scientific), High vacuum pump (RZ6,
359 Vacuubrand) with a glass vacuum manifold and a cold finger, Combiflash purification system (Teledyne
360 ISCO), pH 0-11 test paper (Labomoderne), CEM Discover Bio (manual microwave peptide synthesizer,
361 CEM Corporation), CEM Liberty Blue (automated microwave peptide synthesizer, CEM Corporation),
362 CEM polypropylene SPS reaction vessel (25 mL, CEM Corporation), plastic syringes (1, 2 and 5 mL),
363 micropipette (100 μ L, Eppendorf), frit column plate (Roland vetter laborbedarf OHG), Eppendorf tube
364 (1.5 mL), falcon centrifuge tube (15 mL), centrifuge (Mega star 600R, VWR), vortex mixer (Top mix FB
365 15024, Fisher scientific), freeze dryer (VirTis BenchTop Pro, SP Scientific) with a vacuum pump (RC6,
366 Vacuubrand), flask shaker (SF1, Stuart). RP-HPLC (reverse phase high performance liquid
367 chromatography) to check purity was carried out on a Macherey-Nagel Nucleodur 100-3 C₁₈ec column
368 (3 μ m, 100 x 4 mm) at a flow rate of 1 mL/min with a binary eluent system (solvent A: MilliQ water
369 containing 0.1 % (v/v) TFA and solvent B: acetonitrile containing 0.1 % (v/v) TFA).

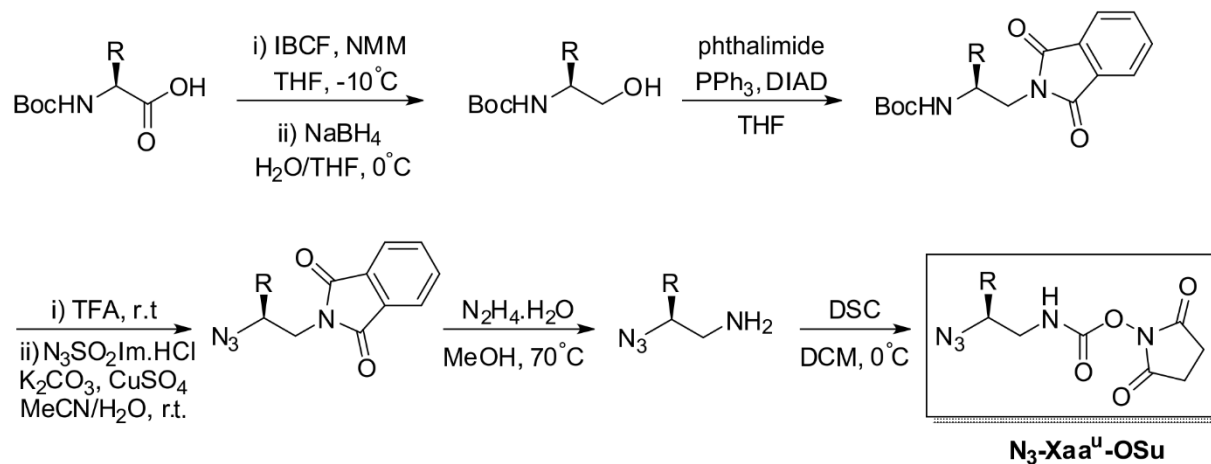
370 5.2 Monomer preparation

371 5.2.1 Azide type monomers bearing the side chain at the β C position (*N*₃-Xaa^u-OSu)

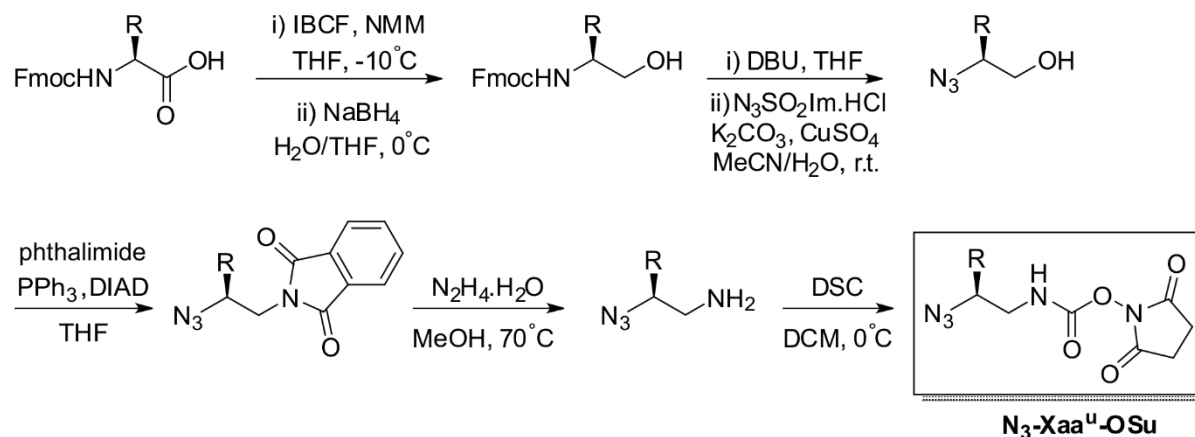
372 The azide-type monomers bearing proteinogenic side chains are synthesized in 6 steps from the
373 corresponding α -amino acids as starting material, as described in the general scheme (Fig. 5). Two

374 pathways have been developed depending on the nature of the side chain: path A is recommended
 375 for monomers without acid labile protecting group on the side chain; path B should be followed
 376 otherwise. These monomers are usually synthesized in our laboratory on a 20 to 30 mmol scale.

path A



path B



377

378 **Fig. 5.** General synthetic procedure for the preparation of azide type monomers bearing side chain at
 379 the β C position, depending on the nature of the side chain.

380

381 *5.2.1.1 Procedure for the preparation of N-protected β -amino alcohol*

382 **Timing:** 8 h.

- 383 1. *N*-Boc (or Fmoc) α -amino acid was dissolved in anhydrous THF (at 0.5 M) under N₂ atmosphere
384 and the solution was cooled down to -20 °C (in salt-ice bath). After addition of NMM (1.2
385 equiv.) and IBCF (1.2 equiv.), the mixture was stirred at -10 °C, for 30 min.
- 386 2. The resulting white suspension was then filtered off and washed with THF twice. The filtrate
387 and washing solution were combined and added to a solution of NaBH₄ (1.2 equiv., 1.0 M) in
388 water at 0 °C. The resulting mixture was stirred at room temperature for 2 h.
- 389 3. The reaction mixture was then quenched by adding a 1 M KHSO₄ solution. The THF was
390 removed using rotary evaporation and the crude was dissolved in EtOAc. After phase
391 separation, two additional extractions of the aqueous phase were performed with EtOAc. The
392 organic layers were then combined and washed twice with a 1 M KHSO₄ solution, then twice
393 with a saturated solution of NaHCO₃ followed by brine. The organic layer was then dried over
394 MgSO₄ and concentrated under reduced pressure to give the corresponding alcohol.

395 **Note:** The addition of THF filtrate to aqueous NaBH₄ solution is accompanied by releasing of hydrogen
396 gas.

397 5.2.1.2 Procedure for the conversion of the alcohol into the corresponding phthalimide

398 **Timing:** 12 -24 h.

399 **Note:** If you are following path B, the **section 5.2.1.3** should be performed before **5.2.1.2**.

- 400 4. Triphenylphosphine (1.2 equiv.) and phthalimide (1.2 equiv.) were dissolved in anhydrous THF
401 (0.3 M), followed by dropwise addition of DIAD (1.2 equiv.) at 0°C under N₂ atmosphere. The
402 mixture was stirred for 10 min.
- 403 5. *N*-Boc protected β -amino alcohol (in path A) (1.0 equiv.) or β -azido alcohol (in path B) (1.0
404 equiv.) was dissolved in anhydrous THF (0.5 M).
- 405 6. The THF solution in step 5 was added to the reaction mixture at 0°C and then the reaction was
406 allowed to reach room temperature.

407 7. The reaction takes 2 h to overnight to go to completion (monitored by TLC). After completion,
408 THF was evaporated under reduced pressure and the crude material was purified by flash
409 chromatography.

410 5.2.1.3 Procedure for the introduction of the azido group

411 **Timing:** 1 day.

412 8. This step aims removing the protecting group on the amine. Please choose the suitable
413 conditions according to the protecting group of the starting α -amino acid.

414 *Option A (removal of Boc group, path A):* The *N*-Boc protected β -amino phthalimide (1.0 equiv.)
415 was dissolved in pure TFA and reaction was stirred at room temperature for 1 hour. Crude was
416 concentrated and directly used in the next step.

417 *Option B (removal of Fmoc group, path B):* The *N*-Fmoc protected β -amino alcohol (1.0 equiv.)
418 was dissolved in THF (0.2 M) followed by addition of DBU (1.1 equiv.). After 1 hour, the solvent
419 was concentrated and crude was directly used in the next step.

420 9. The free amine or the corresponding TFA ammonium salt previously obtained was dissolved in
421 a 1:1 mixture of MeCN / H₂O (0.1 M). K₂CO₃ (\geq 1.5 equiv.), CuSO₄·5H₂O (0.01 equiv.) and
422 N₃SO₂Im·HCl (1.2 equiv.) were added. Reaction was then stirred overnight at room
423 temperature.

424 10. MeCN was evaporated and EtOAc was added to the remaining aqueous layer. The two layers
425 were separated and the aqueous phase was extracted four times with EtOAc. Combined
426 organic layers were washed with a 1 M KHSO₄ solution three times and one time with brine.
427 The organic layer was then dried over MgSO₄ and concentrated under reduced pressure. The
428 azide compound was then purified using flash column chromatography.

429 **Caution:** TFA is corrosive!!! Evaporation of TFA should be carried out on acid resistant equipment.

430 **Note 1:** The diazotransfer reagent Imidazole-1-sulfonyl azide hydrochloride ($N_3SO_2Im \cdot HCl$) is prepared
431 according to the literature(Goddard-Borger & Stick, 2007). **Caution** should be taken when preparing
432 and handling this reagent(Goddard-Borger & Stick, 2011).

433 **Note 2:** In step 9, the amount of K_2CO_3 should be adjusted to neutralize all the acid in the reaction
434 mixture until a pH greater than 8 is reached.

435 *5.2.1.4 Procedure for the removal of the phthalimide group*

436 **Timing:** 8h.

437 11. To a solution of the phthalimide derivative in MeOH (0.1 M) was added hydrazine hydrate (3
438 equiv.). The reaction mixture was heated to reflux and heating was maintained for 4 h.

439 12. The white precipitate was filtered off and MeOH was evaporated using rotary evaporation.
440 The remaining mixture was dissolved in EtOAc and precipitate was removed by filtration. The
441 filtrate was extracted twice with a 1 M $KHSO_4$ solution from the organic phase, and the
442 combined aqueous layers were washed twice with EtOAc.

443 13. Solid K_2CO_3 was then carefully added to the aqueous phase until pH 8 is reached. The basic
444 amine is finally extracted with DCM four times, dried over $MgSO_4$ and concentrated under
445 reduced pressure.

446 **Caution:** The monomers corresponding to Ala, Val and Leu side chains are volatile, do not concentrate
447 to dryness.

448 *5.2.1.5 Procedure for the preparation of succinimidyl azido-2-substituted-ethyl-carbamates*

449 **Timing:** 5h.

450 14. Disuccinimidyl carbonate (1.1 equiv.) dissolved in anhydrous DCM (0.3 M) was cooled to $0^\circ C$.
451 The amine obtained from the previous step was solubilized in anhydrous DCM (0.2 M) and
452 added dropwise to the disuccinimidyl carbonate solution. Reaction was then stirred for 3 hours
453 and allowed to reach room temperature.

454 15. After removal of DCM under rotary evaporation, the crude material was diluted in EtOAc,
455 washed twice with a 1 M KHSO₄ solution and once with brine. The organic layer was dried over
456 MgSO₄ and concentrated under reduced pressure.

457 16. The expected monomer was recovered as a solid after precipitation in a mixture Et₂O/pentane.

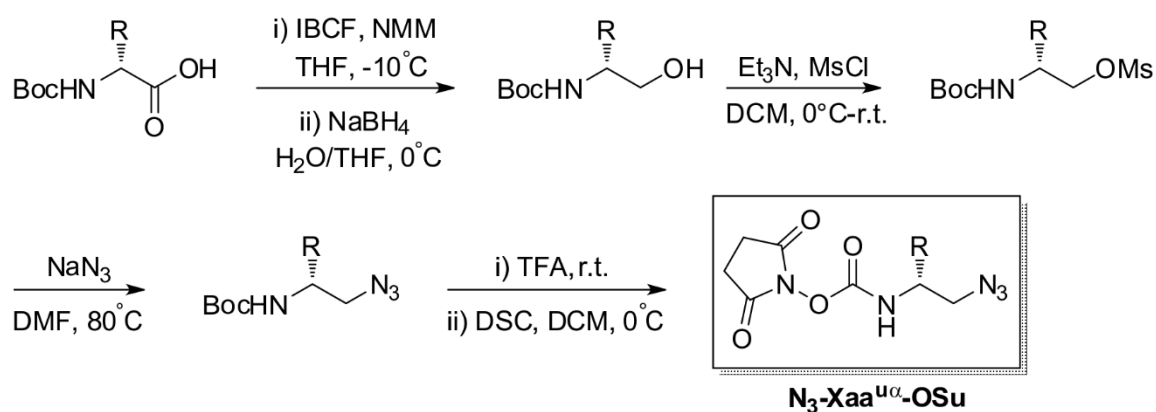
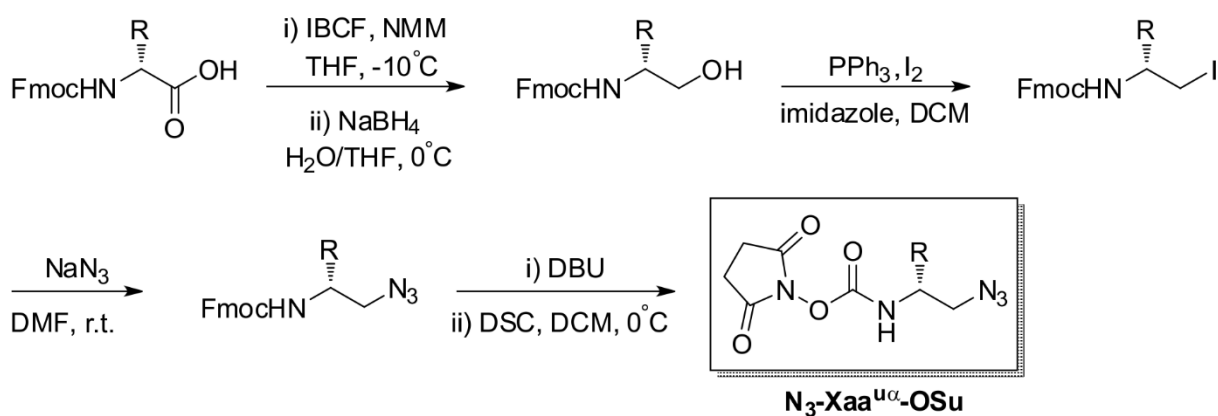
458 5.2.1.6 Example of monomer characterization

459 **N₃-Leu^u-OSu** : mp 92-94°C; [α]_D²⁵ +49.3; t_R = 7.25 min (gradient 10 to 100% of MeCN in H₂O over 10
460 min); ¹H NMR (CDCl₃, 300 MHz) δ 5.69 (t, J = 6.0, 1H), 3.65 – 3.56 (m, 1H), 3.46 (ddd, J = 13.9, 6.8, 3.7,
461 1H), 3.14 (ddd, J = 13.8, 8.2, 5.4, 1H), 2.83 (s, 4H), 1.87 – 1.70 (m, 1H), 1.51 (ddd, J = 14.6, 8.5, 6.2, 1H),
462 1.35 (ddd, J = 13.9, 8.1, 5.6, 1H), 0.96 (d, J = 6.6, 6H); ¹³C NMR (CDCl₃, 75 MHz) δ 169.97, 151.77, 60.12,
463 45.73, 40.74, 25.58, 25.00, 22.92, 22.19; HRMS (ESI-TOFMS) *m/z* calcd for C₁₁H₁₇N₅O₄Cl [M+Cl]⁻
464 318.0969, found 318.0978.

465 <Insert Table 1 here>

466 5.2.2 Azide type monomers bearing the side chain at the α C position (N₃-Xaa^{u α} -OSu)

467 Two synthetic routes are used to prepare these α -substituted monomers, starting either from Boc-
468 protected or Fmoc-protected amino acids (Fig. 6). Path A corresponds to the synthesis using Boc-
469 protected amino acids which are recommended for monomer without acid labile protective groups on
470 the side chain. Path B should be used otherwise. Both synthetic routes are robust, even if a flash
471 column chromatography has to be used to remove impurities after the deprotection step with DBU for
472 the path B, while a simple precipitation is required for the path A.

path A**path B**

473

474 **Fig. 6.** General synthetic procedure for the preparation of azide type monomers bearing side chain at
 475 the ^αC position with inversion of stereochemistry, depending on the nature of the side chain.

476

477 It is worth noting that substituting monomers whose side chain has been shifted to the ^αC for canonical
 478 monomers (*i.e.* monomers bearing the side chain at the ^βC) at discrete positions in an oligoureia
 479 sequence is compatible with helix formation, provided that the two classes of monomers have
 480 opposite absolute configuration. Hence, the synthesis of Xaa^{uα} should start with α-amino acids of (*D*)
 481 configuration if the other Xaa^u monomers of the sequence have been prepared from α-amino acids of
 482 (*L*) configuration.

483 **5.2.2.1 Procedure for the preparation of *N*-protected β-amino alcohol**

484 **Timing:** 8 h

485 As previously described in **section 5.2.1.1**.

486 *5.2.2.2 Procedure for the mesylation of N-Boc- β -amino alcohol (path A)*

487 **Timing:** 24 h

488 17. The *N*-Boc protected β -amino alcohol (1.0 equiv.) was dissolved in DCM (0.5 M) and cooled to
489 0°C under Ar. Et₃N (2.0 equiv.) was added and the mixture was stirred for 15 min at 0°C. Then
490 MsCl (1.1 equiv.) was added dropwise at 0°C and reaction mixture was allowed to reach room
491 temperature and let to react overnight.

492 18. After removal of DCM by rotary evaporation, the crude material was diluted in EtOAc, washed
493 successively twice with a 1 M KHSO₄ solution and once with brine, dried over MgSO₄ and
494 concentrated under reduced pressure to afford the *N*-Boc protected β -amino
495 methanesulfonate derivative.

496 *5.2.2.3 Procedure for the preparation of tert-butyl (2-azido-1-substituted-ethyl)carbamate (Path A)*

497 **Timing:** 8 h

498 19. The *N*-Boc protected β -amino methanesulfonate derivative (1.0 equiv.) was dissolved in DMF
499 (0.4 M). After addition of NaN₃ (5.0 equiv.), reaction mixture was heated to 80°C and stirred
500 for 5 h.

501 20. The reaction medium was then diluted with EtOAc, washed four times with water and once
502 with brine. Organic layer was then dried over MgSO₄ and concentrated under reduced
503 pressure. The *tert*-butyl (2-azido-1-substituted-ethyl)carbamate was obtained as a white solid
504 after high vacuum drying.

505 *5.2.2.4 Procedure for the preparation of succinimidyl (2-azido-1-substituted-ethyl)-carbamates (Path*
506 *A)*

507 **Timing:** 24 h

508 21. The *tert*-butyl (2-azido-1-substituted-ethyl)carbamate (1.0 equiv.) was dissolved in pure TFA
509 and let to react 30 min.

510 22. TFA was removed using rotary evaporation, then the crude material was carefully neutralized
511 using a saturated solution of NaHCO₃.

512 23. The amine compound was then extracted using EtOAc five times. The combined organic layers
513 were dried over MgSO₄ and concentrated under reduced pressure to give the expected amine
514 which was then directly used in the next step.

515 24. As previously described in **section 5.2.1.5**, the expected monomer was obtained as a solid.

516 **Caution:** TFA is corrosive!!! Evaporation of TFA should be carried out on acid resistant equipment.

517 *5.2.2.5 Procedure for the preparation of N-Fmoc β-iodoamine derivative (Path B)*

518 **Timing:** 8 h

519 25. I₂ (3.0 equiv.), PPh₃ (3.0 equiv.) and imidazole (5.0 equiv.) were dissolved in DCM (1.0 M) and
520 flushed with N₂.

521 26. *N*-Fmoc protected β-amino alcohol was dissolved in DCM (1.0 M) and added to the reaction
522 mixture. Reaction was then stirred for 5 h.

523 27. The reaction medium was then washed twice with an aqueous solution of Na₂S₂O₃ (0.5 M) and
524 once with brine. After flash column chromatography, the *N*-Fmoc β-iodoamine derivative
525 compound was recovered as a solid and used directly in the next step.

526 *5.2.2.6 Procedure for preparation of N-Fmoc- amino azide compound (Path B)*

527 **Timing:** 8 h

528 28. The *N*-Fmoc protected β-iodoamine (1.0 equiv.) was dissolved in DMF (0.4 M). After addition
529 of NaN₃ (5.0 equiv.), reaction mixture was stirred for 5 h at room temperature.

530 29. The reaction medium was then diluted with EtOAc, washed four times with water and once
531 with brine. Organic layer was then dried over MgSO₄ and concentrated under reduced
532 pressure. No silica gel purification was required. The *N*-Fmoc protected amino azide was
533 obtained as a solid after high vacuum drying.

534 *5.2.2.7 Procedure for the preparation of succinimidyl 2-azido-1-substituted-ethyl-carbamates (Path B)*

535 **Timing:** 24 h

536 30. (9*H*-fluoren-9-yl)methyl (2-azido-1-substituted-ethyl)carbamate was dissolved in EtOAc (0.1
537 M) and DBU (1.0 equiv.) was added. Reaction mixture was then stirred for 1 h.

538 31. The crude material was concentrated and purified by flash chromatography (100% EtOAc
539 followed by DCM/MeOH/Et₃N 90:8:2). The expected amine was recovered and directly used
540 in the next step.

541 32. Follow the description in **section 5.2.1.5** to give expected building blocks as a solid.

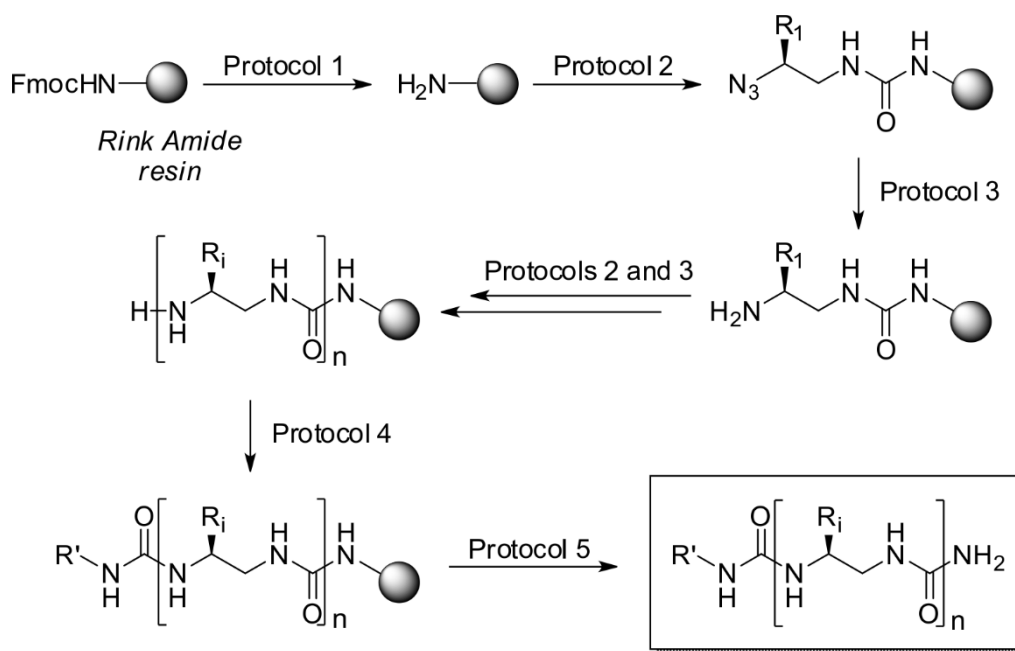
542 <Insert Table 2 here>

543 **5.3 Synthesis of oligourea based foldamers on solid support**

544 The methodology developed to synthesize water soluble oligourea based foldamers on solid support
545 (homo-oligourea as well as hybrid peptide-oligourea or oligourea-peptide sequences) using azide-type
546 monomers is reported here.

547 **5.3.1 Solid phase synthesis of oligoureas**

548 The synthesis of an amphiphilic oligourea foldamer designed to self-assemble in aqueous solution (**H1**
549 : *iPr*^u*L*^u*E*^u*K*^u*L*^u*Y*^u*L*^u*E*^u*K*^u*L*^u*A*^u*L*^u) (Collie et al., 2015) is exemplified on a 50 μmol scale (Fig. 7). Microwave
550 assisted protocols (from 1 to 4) are carried out under N₂ atmosphere using CEM Discover Bio system
551 equipped with a fiber optic sensor for temperature control. In our experience, the protocols can be
552 applied up to 150 μmol scale with consistent efficiency.



553

554 **Fig. 7.** General synthetic procedure for SPS of oligourea foldamers.

555

556 *5.3.1.1 Protocol 1 : Fmoc deprotection to activate the resin*

557 **Timing:** 2 h 10 min

558 1. Add 96 mg of Rink Amide MBHA resin (50 μmol for 0.52 mmol·g⁻¹ loading) to the CEM
559 polypropylene SPS reaction vessel.

560 2. Add 2 mL of DMF to the dried resin and wait 2 h for resin swelling.

561 3. Remove the solvent by filtration, add 3 mL of 20% piperidine/DMF (v/v), and then flush with
562 N₂.

563 4. Place the reaction vessel inside the microwave reactor and irradiate with microwaves (50 W
564 maximum power, ramp to 50°C, with 8 min hold time).

565 5. Take reaction vessel out of microwave reactor, filter the resin, and then wash the resin with
566 DMF (3 x 3 mL).

567 *5.3.1.2 Protocol 2 : Azide-type monomer coupling*

568 **Timing:** 1 h

569 6. Add 75 μmol of $\text{N}_3\text{-Xaa}^{\text{u}}\text{-OSu}$ (1.5 equiv. relative to resin loading) to the 1.5 mL Eppendorf tube
570 followed by adding 26 μL of DIEA (3 equiv. relative to resin loading) and 1.5 mL of DMF.

571 7. Sonicate and vortex the Eppendorf tube to solubilize $\text{N}_3\text{-Xaa}^{\text{u}}\text{-OSu}$ well.

572 8. Transfer the $\text{N}_3\text{-Xaa}^{\text{u}}\text{-OSu}$ solution to the reaction vessel, rinse the Eppendorf tube with 1.5 mL
573 of DMF to transfer residual solution to the reaction vessel, and then flush the reaction vessel
574 with N_2 .

575 9. Place the reaction vessel inside the microwave reactor and irradiate with microwaves (25 W
576 maximum power, ramp to 70°C , with 20 min hold time).

577 10. Take reaction vessel out of the microwave reactor, filter the resin, and then wash the resin
578 successively with DMF (3 mL), DCM (3 x 3 mL) and DMF (2 x 3 mL).

579 11. Repeat Steps 6. to 10. once more.

580 **Note:** The completion of the coupling step can be assessed using a colorimetric test (chloranil
581 test(Vojkovsky, 1995). The absence of free amino function should give a negative result with the resin
582 beads being colorless.

583 *5.3.1.3 Protocol 3 : Azide reduction*

584 **Timing:** 50 min

585 12. Wash the resin with a 70% 1,4-dioxane/water solution (v/v) (2 x 3 mL).

586 13. Add 0.5 mL of 1 M trimethylphosphine in THF solution (10 equiv. relative to resin loading) to
587 the resin followed by adding 2 mL of a 70% 1,4-dioxane/water solution (v/v), and then flush
588 the reaction vessel with N_2 .

589 14. Place the reaction vessel inside the microwave reactor and irradiate with microwaves (25 W
590 maximum power, ramp to 70°C , with 15 min hold time).

591 15. Take reaction vessel out of microwave reactor, filter the resin, and then wash the resin with
592 70% 1,4-dioxane/water (v/v) (2 x 3 mL) and DMF (3 x 3 mL).

593 16. Repeat Steps 12. to 15. once more.

594 *5.3.1.4 Protocol 4 (optional): isopropyl urea capping of the N-terminal amine*

595 **Timing:** 40 min

596 17. Add 15 μ L of isopropyl isocyanate (3 equiv. relative to resin loading) to the 1.5 mL Eppendorf
597 tube followed by adding 44 μ L of DIEA (5 equiv. relative to resin loading) and 1.5 mL of DMF.

598 18. Transfer the solution to the reaction vessel, rinse the Eppendorf tube with 1.5 mL of DMF to
599 transfer residual solution to the reaction vessel, and then flush the reaction vessel with N₂.

600 19. Place the reaction vessel inside the microwave reactor and irradiate with microwaves (25 W
601 maximum power, ramp to 70°C, with 10 min hold time).

602 20. Filter the resin and wash successively with DMF (3 mL), DCM (3 x 3 mL) and DMF (2 x 3 mL).

603 21. Repeat Steps 17. to 20. once more.

604 *5.3.1.5 Protocol 5: Cleavage of the oligourea from the resin*

605 **Timing:** 3 - 8 h

606 22. Transfer the resin into a 5 mL plastic syringe with a frit column plate and wash the resin with
607 DCM (5 x 3 mL).

608 23. Close syringe with a cap, add 3 mL of the cleavage cocktail (TFA/TIS/H₂O=95/2.5/2.5 (v/v/v))
609 to the resin, and then gently close the syringe with its plunger.

610 24. Shake the syringe for 2h using mechanical shaker.

611 25. Filter the cleavage mixture to a round bottomed flask and rinse the resin with cleavage cocktail
612 (2 x 0.5 mL).

613 26. Concentrate the combined filtrate in the round bottomed flask on a rotary evaporator with a
614 bath temperature of 40°C to obtain a viscous oil.

615 27. Add 5 mL of Et₂O into the oil to precipitate, and triturate the precipitate.

616 28. Transfer the mixture to a centrifugal tube and rinse the flask with Et₂O (2 x 3 mL) to transfer
617 residual mixture.

618 29. Centrifuge the mixture for 5 min with 4000 rpm and remove the supernatant.

619 30. Add 10 mL of Et₂O to disperse the precipitate, repeat Step 29. and dry the solid on a vacuum
620 manifold.

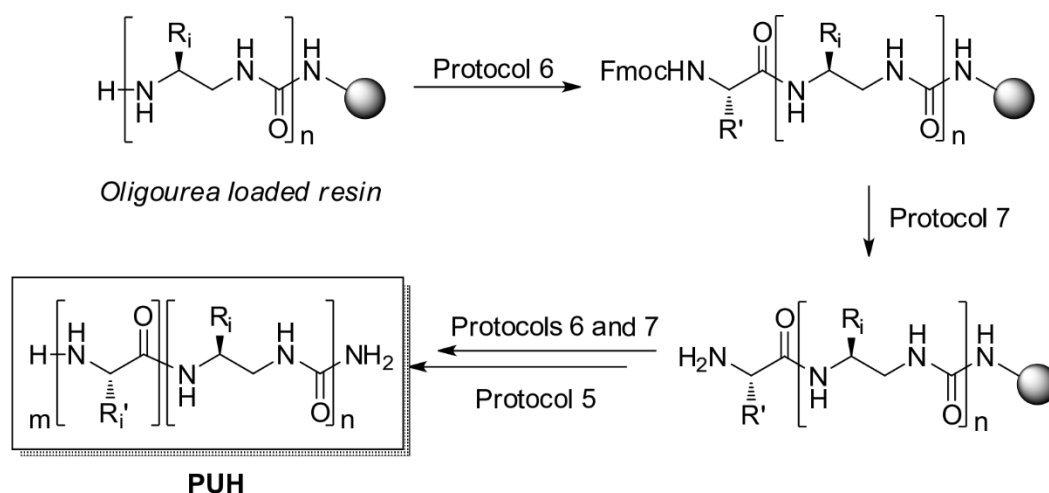
621 31. Dissolve the solid in 20% acetonitrile/water (v/v), and freeze-dry it.

622 **Note 1:** The cleavage time at Step 24. can vary from 2 hours to 6 hours depending on sequences.

623 **Note 2:** Solid-phase synthesis (assembly on the resin and cleavage) of **H1** was typically completed
624 within 28 working hours.

625 **5.3.2 Solid phase synthesis of hybrid peptide-oligourea (PUH) or oligourea-peptide (UPH) sequences**

626 The synthesis of an amphiphilic peptide-oligourea block co-foldamer designed to self-assemble (**PUH** :
627 ALKEIAYAL^uE^uE^uL^uQ^uL^u) is exemplified here on a 50 μmol scale (Fig. 8). The elongation of the peptide
628 part of the hybrid sequences is accomplished under N₂ atmosphere using automated solid phase
629 peptide synthesizer with microwaves assistance (CEM Liberty Blue system) equipped with a fiber optic
630 sensor for temperature control. The peptide part can be incorporated regardless of its position in the
631 sequence (before (e.g. **UPH**), after (e.g. **PUH**) or between the oligourea part). For the oligourea
632 segment, the same protocols as described in the previous section are used. In our experience, the
633 protocols can be applied up to 150 μmol scale with consistent efficiency.



634

PUH

635 **Fig. 8.** General synthetic procedure for SPS of peptide-oligourea hybrid foldamers (**PUH**).

636

637 *5.3.2.1 Protocol 6: Peptide coupling*

638 **Timing:** 5 min

639 32. Add 1.5 mL of 0.2 M Fmoc- α -Xaa-OH in DMF (6 equiv. relative to resin loading) to the resin
 640 followed by adding 0.6 mL of 0.5 M DIC in DMF (6 equiv. relative to resin loading) and 0.3 mL
 641 of 1 M Oxyma in DMF (6 equiv. relative to resin loading).

642 33. Irradiate with microwaves (170 W maximum power, ramp to 75°C, with 15 s hold time + 30 W
 643 maximum power, ramp to 90°C, with 110 s hold time)

644 34. Filter the resin and wash with DMF (2 mL).

645 35. Repeat steps 32. to 34. once more

646 *5.3.2.2 Protocol 7: Fmoc deprotection*

647 **Timing:** 5 min

648 36. Add 3 mL of 20% piperidine/DMF (v/v) to the resin

649 37. Irradiate with microwaves (155 W maximum power, ramp to 75°C, with 15 s hold time + 30 W
 650 maximum power, ramp to 90°C, with 50 s hold time)

651 38. Filter the resin and wash with DMF (2 x 2 mL and 3 mL)

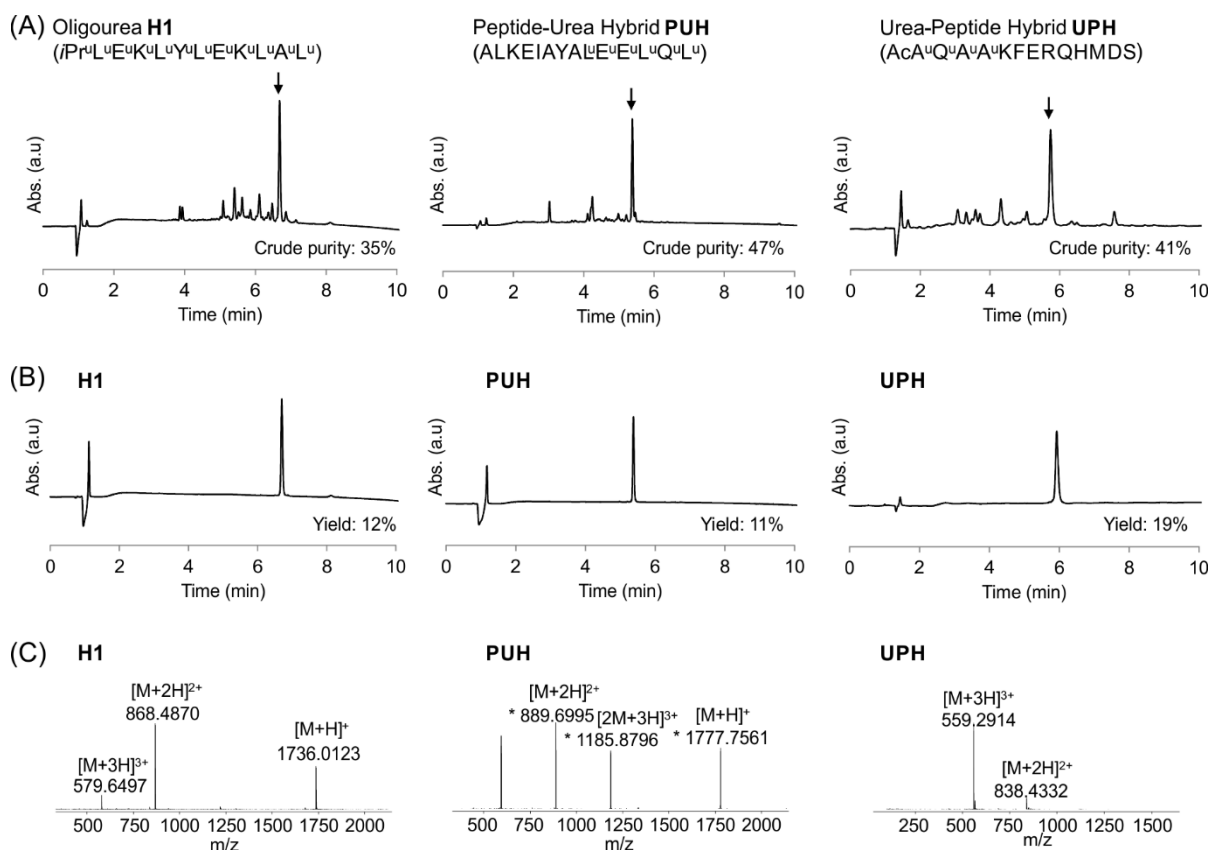
652 **Note:** Automated-assisted synthesis (assembly on the resin and cleavage) of **PUH** and **UPH** was
653 typically completed within 16-20 working hours.

654

655 **5.3.3 Purification and characterization of oligourea-based foldamers**

656 Analytical RP-HPLC (Fig. 9A-B) and LC-MS (liquid chromatography-mass spectrometry) (Fig. 9C) are
657 used to evaluate the purity of the crude product and confirm the identity of the expected compound
658 after cleavage from the resin.

659 Purification via preparative RP-HPLC is performed on a Macherey-Nagel Nucleodur 100-5 C₁₈HTec
660 column (5 μm, 250 x 21 mm) at a flow rate of 20 mL/min with the same binary eluent system as
661 analytical RP-HPLC. Gradients and running time were optimized for each sequence. For example, **H1** is
662 purified using a gradient of 30% to 70% solvent B over 20 min. In addition to the primary
663 characterization using mass spectrometry, conformational analysis and structural characterization in
664 solution or solid state can be accomplished using NMR, CD, crystallography and others.



665

666 **Fig. 9.** Analytical HPLC profiles (A) before, and (B) after purification. (C) mass spectrometry analysis of
 667 foldamers **H1**, **PUH** and **UPH**. Crude purities are determined from peak area percentages. Arrows in
 668 (A) indicate peaks corresponding to the desired products. Gradients of 15% to 30% solvent B were
 669 applied for analytical HPLC of **UPH** while the standard gradient of 10% to 100% solvent B were applied
 670 for **H1** and **PUH**.

671

672 5.3.4 Troubleshooting

673 The above-mentioned protocols generally result in good to high crude purities as shown in Fig. 9A.

674 However, in the specific case of oligourea-peptide hybrids (in contrast to peptide-oligourea hybrids),

675 we observed that some sequences yield poor results with a low purity of the crude product. A more

676 detailed analysis following intermediate cleavage at different steps of the synthesis reveals the

677 formation of a byproduct after each azide reduction step, whose mass is higher than the expected

678 amine by a value of 26 Da. The current hypothesis based on NMR and MS analysis is that a competitive

679 cyclization occurs concomitantly with the reduction leading to a biuret formation, which ends further

680 elongation of the sequence. Varying either the nature of the phosphine or the protecting group of the

681 monomer (e. g. using Fmoc-protected monomer instead of azido-type) may help improving the overall

682 efficiency of the synthesis. Investigations are currently ongoing to better identify sequences that may
683 cause problems, and develop a more robust protocol for such “difficult” sequences.

684

685 **6. CONCLUDING REMARKS AND FUTURE DIRECTIONS**

686 The access to a large repertoire of monomeric units whose molecular diversity extends beyond that of
687 proteinogenic side chains, together with robust automated SPS methods have been instrumental in
688 the development of oligourea foldamers and their applications (molecular recognition, catalysis,
689 disruption of PPI, ...). The combination of automation and microwave assistance considerably reduces
690 the duration of the synthesis while enabling parallel synthesis and access to foldamer libraries.
691 Moreover, the possibility to generate chimeric helices by combining peptide and oligourea backbones
692 in a single strand further expands the range of applications of oligoureas as α -helix mimics. Although
693 the reported protocols allow smooth syntheses of a large number of homooligourea and hybrid
694 sequences, we identified some “difficult sequences” while preparing oligourea-peptide chimeras.
695 Continuous improvement of the synthesis of hybrid foldamer-peptide sequences is justified by the
696 recent finding that the replacement of a short α -helical segment within a bioactive peptide by an
697 oligourea insert may yield peptide analogues with increased resistance to proteolytic degradation and
698 prolonged duration of action *in vivo*. Finally, oligourea chemistry is versatile enough to be combined
699 with other known peptide stabilization methods such as macrocyclization or lipidation to further
700 increase helical content and potency of bioactive peptides.

701 **ACKNOWLEDGEMENTS**

702 This work was supported by the Agence Nationale de la Recherche (ANR) grants ANR-15-CE07-0010,
703 ANR-17-CE07-0020 and ANR-18-CE07-0018-01. Postdoctoral fellowships to S.H.Y. from IdEx Bordeaux
704 (ANR-10-IDEX-03-02), a program of the French government managed by ANR and to B.L. from the
705 Conseil Régional de Nouvelle-Aquitaine (2017-1R10115) are gratefully acknowledged. We also thank
706 Ureka Pharma for generously supporting our research in the field of urea oligomers.

707

708 **REFERENCES**

- 709 Antunes, S., Douat, C., & Guichard, G. (2016). Solid-Phase Synthesis of Hybrid Urea Oligomers
710 Containing Conservative Thiourea Mutations. *European Journal of Organic Chemistry*,
711 *2016(12)*, 2131-2138. doi:10.1002/ejoc.201600177
- 712 Azzarito, V., Long, K., Murphy, N. S., & Wilson, A. J. (2013). Inhibition of [alpha]-helix-mediated protein-
713 protein interactions using designed molecules. *Nature Chemistry*, *5(3)*, 161-173.
714 doi:10.1038/nchem.1568
- 715 Bécart, D., Diemer, V., Salaün, A., Oiarbide, M., Nelli, Y. R., Kauffmann, B., et al. (2017). Helical
716 Oligourea Foldamers as Powerful Hydrogen Bonding Catalysts for Enantioselective C-C Bond-
717 Forming Reactions. *Journal of the American Chemical Society*, *139(36)*, 12524-12532.
718 doi:10.1021/jacs.7b05802
- 719 Boersma, M. D., Haase, H. S., Peterson-Kaufman, K. J., Lee, E. F., Clarke, O. B., Colman, P. M., et al.
720 (2011). Evaluation of Diverse α/β -Backbone Patterns for Functional α -Helix Mimicry:
721 Analogues of the Bim BH3 Domain. *Journal of the American Chemical Society*, *134(1)*, 315-323.
722 doi:10.1021/ja207148m
- 723 Bornerie, M., Brion, A., Guichard, G., Kichler, A., & Douat, C. (2021). Delivery of siRNA by tailored cell-
724 penetrating urea-based foldamers. *Chemical Communications*. doi:10.1039/D0CC06285E
- 725 Burgess, K., Shin, H., & Linthicum, D. S. (1995). Solid-Phase Syntheses of Unnatural Biopolymers
726 Containing Repeating Urea Units. *Angewandte Chemie - International Edition*, *34(8)*, 907-909.
727 doi:10.1002/anie.199509071
- 728 Checco, J. W., & Gellman, S. H. (2016). Targeting recognition surfaces on natural proteins with peptidic
729 foldamers. *Current Opinion in Structural Biology*, *39*, 96-105. doi:10.1016/j.sbi.2016.06.014
- 730 Checco, J. W., Lee, E. F., Evangelista, M., Sleebs, N. J., Rogers, K., Pettikiriachchi, A., et al. (2015). α/β -
731 Peptide Foldamers Targeting Intracellular Protein-Protein Interactions with Activity in Living

732 Cells. *Journal of the American Chemical Society*, 137(35), 11365-11375.
733 doi:10.1021/jacs.5b05896

734 Cheloha, R. W., Maeda, A., Dean, T., Gardella, T. J., & Gellman, S. H. (2014). Backbone modification of
735 a polypeptide drug alters duration of action in vivo. *Nature Biotechnology*, 32(7), 653-655.
736 doi:10.1038/nbt.2920

737 Claudon, P., Violette, A., Lamour, K., Decossas, M., Fournel, S., Heurtault, B., et al. (2010).
738 Consequences of Isostructural Main-Chain Modifications for the Design of Antimicrobial
739 Foldamers: Helical Mimics of Host-Defense Peptides Based on a Heterogeneous Amide/Urea
740 Backbone. *Angewandte Chemie - International Edition*, 49(2), 333-336.
741 doi:10.1002/anie.200905591

742 Collie, G. W., Bailly, R., Pulka-Ziach, K., Lombardo, C. M., Mauran, L., Taib-Maamar, N., et al. (2017).
743 Molecular Recognition within the Cavity of a Foldamer Helix Bundle: Encapsulation of Primary
744 Alcohols in Aqueous Conditions. *Journal of the American Chemical Society*, 139(17), 6128-
745 6137. doi:10.1021/jacs.7b00181

746 Collie, G. W., Pulka-Ziach, K., & Guichard, G. (2016). In situ iodination and X-ray crystal structure of a
747 foldamer helix bundle. *Chemical Communications (Cambridge)*, 52(6), 1202-1205.
748 doi:10.1039/c5cc07916k

749 Collie, G. W., Pulka-Ziach, K., & Guichard, G. (2016). Surfactant-facilitated crystallisation of water-
750 soluble foldamers. *Chemical Science*, 7(5), 3377-3383. doi:10.1039/c6sc00090h

751 Collie, G. W., Pulka-Ziach, K., Lombardo, C. M., Fremaux, J., Rosu, F., Decossas, M., et al. (2015). Shaping
752 quaternary assemblies of water-soluble non-peptide helical foldamers by sequence
753 manipulation. *Nature Chemistry*, 7(11), 871-878. doi:10.1038/nchem.2353

754 Cussol, L., Mauran-Ambrosino, L., Buratto, J., Belorusova, A. Y., Neuville, M., Osz, J., et al. (2021).
755 Structural Basis for α -Helix Mimicry and Inhibition of Protein-Protein Interactions with
756 Oligourea Foldamers. *Angewandte Chemie International Edition*, 60(5), 2296-2303.
757 doi:doi.org/10.1002/anie.202008992

758 Diemer, V., Fischer, L., Kauffmann, B., & Guichard, G. (2016). Anion Recognition by Aliphatic Helical
759 Oligoureas. *Chemistry - A European Journal*, 22(44), 15684-15692.
760 doi:10.1002/chem.201602481

761 Douat-Casassus, C., Pulka, K., Claudon, P., & Guichard, G. (2012). Microwave-Enhanced Solid-Phase
762 Synthesis of N,N'-Linked Aliphatic Oligoureas and Related Hybrids. *Organic Letters*, 14(12),
763 3130-3133. doi:10.1021/ol3012106

764 Douat, C., Aisenbrey, C., Antunes, S., Decossas, M., Lambert, O., Bechinger, B., et al. (2015). A Cell-
765 Penetrating Foldamer with a Bio-reducible Linkage for Intracellular Delivery of DNA.
766 *Angewandte Chemie - International Edition*, 54(38), 11133-11137.
767 doi:10.1002/anie.201504884

768 Douat, C., Bornerie, M., Antunes, S., Guichard, G., & Kichler, A. (2019). Hybrid Cell-Penetrating
769 Foldamer with Superior Intracellular Delivery Properties and Serum Stability. *Bioconjugate
770 Chemistry*, 30(4), 1133-1139. doi:10.1021/acs.bioconjchem.9b00075

771 Ferrand, Y., & Huc, I. (2018). Designing Helical Molecular Capsules Based on Folded Aromatic Amide
772 Oligomers. *Accounts of Chemical Research*, 51(4), 970-977. doi:10.1021/acs.accounts.8b00075

773 Fischer, L., Claudon, P., Pendem, N., Miclet, E., Didierjean, C., Ennifar, E., et al. (2010). The Canonical
774 Helix of Urea Oligomers at Atomic Resolution. Insight Into Folding-induced Axial Organization.
775 *Angewandte Chemie - International Edition*, 49(6), 1067-1070. doi:10.1002/anie.200905592

776 Fischer, L., & Guichard, G. (2010). Folding and self-assembly of aromatic and aliphatic urea oligomers:
777 Towards connecting structure and function. *Organic & Biomolecular Chemistry*, 8(14), 3101-
778 3117. doi:10.1039/c001090a

779 Fremaux, J., Fischer, L., Arbogast, T., Kauffmann, B., & Guichard, G. (2011). Condensation Approach to
780 Aliphatic Oligourea Foldamers: Helices with N-(pyrrolidin-2-ylmethyl)ureido Junctions.
781 *Angewandte Chemie - International Edition*, 50, 11382-11385. doi:10.1002/anie.201105416

782 Fremaux, J., Kauffmann, B., & Guichard, G. (2014). Synthesis and Folding Propensity of Aliphatic
783 Oligoureas Containing Repeats of Proline-Type Units. *Journal of Organic Chemistry*, 79(12),
784 5494-5502. doi:10.1021/jo5006075

785 Fremaux, J., Mauran, L., Pulka-Ziach, K., Kauffmann, B., Odaert, B., & Guichard, G. (2015). α -Peptide–
786 Oligourea Chimeras: Stabilization of Short α -Helices by Non-Peptide Helical Foldamers.
787 *Angewandte Chemie - International Edition*, 54(34), 9816-9820. doi:10.1002/anie.201500901

788 Fremaux, J., Venin, C., Mauran, L., Zimmer, R., Koensgen, F., Rognan, D., et al. (2019). Ureidopeptide
789 GLP-1 analogues with prolonged activity in vivo via signal bias and altered receptor trafficking.
790 *Chemical Science*, 10(42), 9872-9879. doi:10.1039/C9SC02079A

791 Fremaux, J., Venin, C., Mauran, L., Zimmer, R. H., Guichard, G., & Goudreau, S. R. (2019). Peptide-
792 oligourea hybrids analogue of GLP-1 with improved action in vivo. *Nature Communications*,
793 10(1), 924. doi:10.1038/s41467-019-08793-y

794 Gan, Q., Wang, X., Kauffmann, B., Rosu, F., Ferrand, Y., & Huc, I. (2017). Translation of rod-like template
795 sequences into homochiral assemblies of stacked helical oligomers. *Nature Nanotechnology*,
796 12(5), 447-452. doi:10.1038/nnano.2017.15

797 Gellman, S. H. (1998). Foldamers: A Manifesto. *Accounts of Chemical Research*, 31(4), 173-180.
798 doi:10.1021/ar960298r

799 Goddard-Borger, E. D., & Stick, R. V. (2007). An Efficient, Inexpensive, and Shelf-Stable Diazotransfer
800 Reagent: Imidazole-1-sulfonyl Azide Hydrochloride. *Organic Letters*, 9(19), 3797-3800.
801 doi:10.1021/ol701581g

802 Goddard-Borger, E. D., & Stick, R. V. (2011). An Efficient, Inexpensive, and Shelf-Stable Diazotransfer
803 Reagent: Imidazole-1-sulfonyl Azide Hydrochloride. *Organic Letters*, 13(9), 2514-2514.
804 doi:10.1021/ol2007555

805 Goodman, C. M., Choi, S., Shandler, S., & DeGrado, W. F. (2007). Foldamers as versatile frameworks
806 for the design and evolution of function. *Nature Chemical Biology*, 3(5), 252-262.
807 doi:10.1038/nchembio876

808 Gopalakrishnan, R., Frolov, A. I., Knerr, L., Drury, W. J., & Valeur, E. (2016). Therapeutic Potential of
809 Foldamers: From Chemical Biology Tools To Drug Candidates? *Journal of Medicinal Chemistry*,
810 59(21), 9599-9621. doi:10.1021/acs.jmedchem.6b00376

811 Guichard, G., & Huc, I. (2011). Synthetic foldamers. *Chemical Communications (Cambridge)*, 47(21),
812 5933-5941. doi:10.1039/c1cc11137j

813 Guichard, G., Semetey, V., Didierjean, C., Aubry, A., Briand, J.-P., & Rodriguez, M. (1999). Effective
814 Preparation of O-Succinimidyl-2- (tert-butoxycarbonylamino)ethylcarbamate Derivatives from
815 α -Amino Acids. Application to the Synthesis of Urea-Containing Pseudopeptides and
816 Oligoureas. *Journal of Organic Chemistry*, 64(23), 8702-8705. doi:10.1021/jo990092e

817 Guichard, G., Semetey, V., Rodriguez, M., & Briand, J.-P. (2000). Solid phase synthesis of oligoureas
818 using O-succinimidyl-(9H-fluoren-9-ylmethoxycarbonylamino)ethylcarbamate derivatives as
819 activated monomers. *Tetrahedron Letters*, 41(10), 1553-1557. doi:10.1016/s0040-
820 4039(99)02353-9

821 Horne, W. S., & Grossmann, T. N. (2020). Proteomimetics as protein-inspired scaffolds with defined
822 tertiary folding patterns. *Nature Chemistry*, 12(4), 331-337. doi:10.1038/s41557-020-0420-9

823 Horne, W. S., Johnson, L. M., Ketas, T. J., Klasse, P. J., Lu, M., Moore, J. P., et al. (2009). Structural and
824 biological mimicry of protein surface recognition by α/β -peptide foldamers. *Proceedings of the*
825 *National Academy of Sciences of the United States of America*, 106(35), 14751-14756.
826 doi:10.1073/pnas.0902663106

827 Johnson, L. M., Barrick, S., Hager, M. V., McFedries, A., Homan, E. A., Rabaglia, M. E., et al. (2014). A
828 Potent α/β -Peptide Analogue of GLP-1 with Prolonged Action in Vivo. *Journal of the American*
829 *Chemical Society*, 136(37), 12848-12851. doi:10.1021/ja507168t

830 Johnson, L. M., & Gellman, S. H. (2013). Chapter Nineteen - α -Helix Mimicry with α/β -Peptides. In E. K.
831 Amy (Ed.), *Methods Enzymol.* (Vol. 523, pp. 407-429): Academic Press.

832 Kim, J.-M., Bi, Y., Paikoff, S. J., & Schultz, P. G. (1996). The solid phase synthesis of oligoureas.
833 *Tetrahedron Lett.*, 37(30), 5305-5308.

834 Kritzer, J. A., Hodsdon, M. E., & Schepartz, A. (2005). Solution structure of a [beta]-peptide ligand for
835 hDM2. *Journal of the American Chemical Society*, *127*, 4118-4119. doi:10.1021/ja042933r

836 Kritzer, J. A., Stephens, O. M., Guarracino, D. A., Reznik, S. K., & Schepartz, A. (2005). [beta]-Peptides
837 as inhibitors of protein-protein interactions. *Bioorganic & Medicinal Chemistry*, *13*, 11-16.
838 doi:10.1016/j.bmc.2004.09.009

839 Le Grel, P., & Guichard, G. (2007). Foldamers: Structure, Properties, and Applications. In S. Hecht & I.
840 Huc (Eds.), *Foldamers: Structure, Properties, and Applications* (pp. 35-74). Weinheim: Wiley-
841 VCH.

842 Lee, E. F., Sadowsky, J. D., Smith, B. J., Czabotar, P. E., Peterson-Kaufman, K. J., Colman, P. M., et al.
843 (2009). High-Resolution Structural Characterization of a Helical α/β -Peptide Foldamer Bound
844 to the Anti-Apoptotic Protein Bcl-xL. *Angew. Chem. Int. Ed. Engl.*, *48*(24), 4318-4322.
845 doi:10.1002/anie.200805761

846 Legrand, B., André, C., Wenger, E., Didierjean, C., Averlant-Petit, M. C., Martinez, J., et al. (2012).
847 Robust Helix Formation in a New Family of Oligoureas Based on a Constrained Bicyclic Building
848 Block. *Angewandte Chemie - International Edition*, *51*(45), 11267-11270.
849 doi:10.1002/anie.201205842

850 Liu, S., Cheloha, R. W., Watanabe, T., Gardella, T. J., & Gellman, S. H. (2018). Receptor selectivity from
851 minimal backbone modification of a polypeptide agonist. *Proceedings of the National Academy
852 of Sciences of the United States of America*, *115*(49), 12383-12388.
853 doi:10.1073/pnas.1815294115

854 Liu, S., Jean-Alphonse, F. G., White, A. D., Wootten, D., Sexton, P. M., Gardella, T. J., et al. (2019). Use
855 of Backbone Modification To Enlarge the Spatiotemporal Diversity of Parathyroid Hormone
856 Receptor-1 Signaling via Biased Agonism. *Journal of the American Chemical Society*, *141*(37),
857 14486-14490. doi:10.1021/jacs.9b04179

858 Lombardo, C. M., Collie, G. W., Pulka-Ziach, K., Rosu, F., Gabelica, V., Mackereth, C. D., et al. (2016).
859 Anatomy of an Oligourea Six-Helix Bundle. *Journal of the American Chemical Society*, *138*(33),
860 10522-10530. doi:10.1021/jacs.6b05063

861 Lombardo, C. M., Kumar, V., Douat, C., Rosu, F., Mergny, J. L., Salgado, G. F., et al. (2019). Design and
862 Structure Determination of a Composite Zinc Finger Containing a Nonpeptide Foldamer Helical
863 Domain. *Journal of the American Chemical Society*, *141*(6), 2516-2525.
864 doi:10.1021/jacs.8b12240

865 Mauran, L., Kauffmann, B., Odaert, B., & Guichard, G. (2016). Stabilization of an α -helix by short
866 adjacent accessory foldamers. *Comptes Rendus Chimie*, *19*(1-2), 123-131.
867 doi:10.1016/j.crci.2015.07.003

868 Mbianda, J., Bakail, M., André, C., Moal, G., Perrin, M. E., Guerois, R., et al. (2020). Optimal Anchoring
869 of a Urea-based Foldamer Inhibitor of ASF1 Histone Chaperone Through Backbone Plasticity.
870 *ChemRxiv*, 10.26434/chemrxiv.12624722.v12624721. doi:10.26434/chemrxiv.12624722.v1

871 Michel, J., Harker, E. A., Tirado-Rives, J., Jorgensen, W. L., & Schepartz, A. (2009). In Silico Improvement
872 of beta3-peptide inhibitors of p53 x hDM2 and p53 x hDMX. *Journal of the American Chemical*
873 *Society*, *131*(18), 6356-6357. doi:10.1021/ja901478e

874 Milbeo, P., Simon, M., Didierjean, C., Wenger, E., Aubert, E., Martinez, J., et al. (2020). A bicyclic unit
875 reversal to stabilize the 12/14-helix in mixed homochiral oligoureas. *Chemical*
876 *Communications*, *56*(57), 7921-7924. doi:10.1039/D0CC02902E

877 Nelli, Y.-R., Douat-Casassus, C., Claudon, P., Kauffmann, B., Didierjean, C., & Guichard, G. (2012). An
878 activated building block for the introduction of the histidine side chain in aliphatic oligourea
879 foldamers. *Tetrahedron*, *68*(23), 4492-4500. doi:10.1016/j.tet.2011.11.066

880 Nelli, Y. R., Antunes, S., Salaün, A., Thinon, E., Massip, S., Kauffmann, B., et al. (2015). Isosteric
881 Substitutions of Urea to Thiourea and Selenourea in Aliphatic Oligourea Foldamers: Site-
882 Specific Perturbation of the Helix Geometry. *Chemistry - A European Journal*, *21*(7), 2870-2880.
883 doi:10.1002/chem.201405792

884 Nelli, Y. R., Fischer, L., Collie, G. W., Kauffmann, B., & Guichard, G. (2013). Structural characterization
885 of short hybrid urea/carbamate (U/C) foldamers: A case of partial helix unwinding.
886 *Biopolymers (Pept Sci)* 100(6), 687-697. doi:10.1002/bip.22302

887 Pappas, C. G., Mandal, P. K., Liu, B., Kauffmann, B., Miao, X., Komáromy, D., et al. (2020). Emergence
888 of low-symmetry foldamers from single monomers. *Nature Chemistry*, 12(12), 1180-1186.
889 doi:10.1038/s41557-020-00565-2

890 Pasco, M., Dolain, C., & Guichard, G. (2017). Foldamers in Medicinal Chemistry. In J. L. Atwood (Ed.),
891 *Comprehensive Supramolecular Chemistry II* (Vol. 5, pp. 89–125). Oxford: Elsevier.

892 Pendem, N., Douat, C., Claudon, P., Laguerre, M., Castano, S., Desbat, B., et al. (2013). Helix-Forming
893 Propensity of Aliphatic Urea Oligomers Incorporating Noncanonical Residue Substitution
894 Patterns. *J. Am. Chem. Soc.*, 135(12), 4884-4892. doi:10.1021/ja401151v

895 Pendem, N., Nelli, Y. R., Douat, C., Fischer, L., Laguerre, M., Ennifar, E., et al. (2013). Controlling Helix
896 Formation in the γ -Peptide Superfamily: Heterogeneous Foldamers with Urea/Amide and
897 Urea/Carbamate Backbones. *Angewandte Chemie - International Edition*, 52(15), 4147-4151.
898 doi:10.1002/anie.201209838

899 Pulka-Ziach, K., & Sęk, S. (2017). α -Helicomimetic foldamers as electron transfer mediators. *Nanoscale*,
900 9(39), 14913-14920. doi:10.1039/C7NR05209J

901 Seebach, D., Beck, A. K., & Bierbaum, D. J. (2004). The World of β - and γ -Peptides Comprised of
902 Homologated Proteinogenic Amino Acids and Other Components. *Chemistry & Biodiversity*,
903 1(8), 1111-1239. doi:10.1002/cbdv.200490087

904 Semetey, V., Didierjean, C., Briand, J.-P., Aubry, A., & Guichard, G. (2002). Self-Assembling Organic
905 Nanotubes from Enantiopure Cyclo-N,N'-Linked Oligoureas: Design, Synthesis, and Crystal
906 Structure. *Angewandte Chemie - International Edition*, 41(11), 1895-1898. doi:10.1002/1521-
907 3773(20020603)41:11<1895::AID-ANIE1895>3.0.CO;2-3

908 Semetey, V., Rognan, D., Hemmerlin, C., Graff, R., Briand, J.-P., Marraud, M., et al. (2002). Stable Helical
909 Secondary Structure in Short-Chain N,N'-Linked Oligoureas Bearing Proteinogenic Side Chains.

910 *Angewandte Chemie - International Edition*, 41(11), 1893-1895. doi:10.1002/1521-
911 3773(20020603)41:11<1893::AID-ANIE1893>3.0.CO;2-F

912 Teyssières, E., Corre, J.-P., Antunes, S., Rougeot, C., Dugave, C., Jouvion, G., et al. (2016). Proteolytically
913 Stable Foldamer Mimics of Host-Defense Peptides with Protective Activities in a Murine Model
914 of Bacterial Infection. *Journal of Medicinal Chemistry*, 59(18), 8221-8232.
915 doi:10.1021/acs.jmedchem.6b00144

916 Violette, A., Averlant-Petit, M. C., Semetey, V., Hemmerlin, C., Casimir, R., Graff, R., et al. (2005). N,N'-
917 Linked Oligoureas as Foldamers: Chain Length Requirements for Helix Formation in Protic
918 Solvent Investigated by Circular Dichroism, NMR Spectroscopy, and Molecular Dynamics.
919 *Journal of the American Chemical Society*, 127(7), 2156-2164. doi:10.1021/ja044392b

920 Violette, A., Fournel, S., Lamour, K., Chaloin, O., Frisch, B., Briand, J.-P., et al. (2006). Mimicking Helical
921 Antibacterial Peptides with Nonpeptidic Folding Oligomers. *Chemistry & Biology*, 13(5), 531-
922 538. doi:10.1016/j.chembiol.2006.03.009

923 Vojkovsky, T. (1995). Detection of secondary amines on solid phase. *Pept Res*, 8(4), 236-237.

924 Wechsel, R., Raftery, J., Cavagnat, D., Guichard, G., & Clayden, J. (2016). The meso Helix: Symmetry
925 and Symmetry-Breaking in Dynamic Oligourea Foldamers with Reversible Hydrogen-Bond
926 Polarity. *Angewandte Chemie - International Edition*, 55(33), 9657-9661.
927 doi:10.1002/anie.201604496

928 Wechsel, R., Žabka, M., Ward, J. W., & Clayden, J. (2018). Competing Hydrogen-Bond Polarities in a
929 Dynamic Oligourea Foldamer: A Molecular Spring Torsion Balance. *Journal of the American
930 Chemical Society*, 140(10), 3528-3531. doi:10.1021/jacs.8b00567

931 Wolfe, S. A., Nekludova, L., & Pabo, C. O. (2000). DNA recognition by Cys2His2 zinc finger proteins.
932 *Annual Review of Biophysics and Biomolecular Structure*, 29, 183-212.
933 doi:10.1146/annurev.biophys.29.1.183

934 Yoo, S. H., Collie, G. W., Mauran, L., & Guichard, G. (2020). Formation and Modulation of Nanotubular
935 Assemblies of Oligourea Foldamers in Aqueous Conditions using Alcohol Additives.
936 *ChemPlusChem*, 85(10), 2243-2250. doi:10.1002/cplu.202000373

937

938 TABLES

939 **Table 1.** Azide type monomers bearing side chain at the $^{\beta}\text{C}$ position prepared according to **Figure 4**:
 940 details of pathway and overall yield.

Starting amino acid	Path ^a	Monomer	Yield ^b (%)
Boc-Ala-OH	A	N ₃ -Ala ^u -OSu	21
Boc-Val-OH	A	N ₃ -Val ^u -OSu	25
Boc-Leu-OH	A	N ₃ -Leu ^u -OSu	28
Boc-Ile-OH	A	N ₃ -Ile ^u -OSu	48
Boc-Phe-OH	A	N ₃ -Phe ^u -OSu	31
Fmoc-Lys(Boc)-OH	B	N ₃ -Lys ^u (Boc)-OSu	26
Fmoc-Glu(O ^t Bu)-OH	B	N ₃ -Glu ^u (O ^t Bu)-OSu	37
Fmoc-Gln(Trt)-OH	B	N ₃ -Gln ^u (Trt)-OSu	11
Fmoc-Thr(O ^t Bu)-OH	B	N ₃ -Thr ^u (O ^t Bu)-OSu	16
Fmoc-Tyr(O ^t Bu)-OH	B	N ₃ -Tyr ^u (O ^t Bu)-OSu	20
Fmoc-Trp(Boc)-OH	B	N ₃ -Trp ^u (Boc)-OSu	17
Fmoc-Arg(Pbf)-OH	B	N ₃ -Arg ^u (Pbf)-OSu	22

941 ^aSee **Figure 4**. ^bThe yield corresponds to the overall yield.
 942

943 **Table 2.** Azide type monomers bearing side chain at the $^{\alpha}\text{C}$ position prepared according to **Figure 5**:
 944 details of pathway and overall yield.

Starting amino acid	Path ^a	Monomer	Yield ^b (%)
Boc-(D)-Ala-OH	A	N ₃ -Ala ^{uα} -OSu	28
Boc-(L)-Val-OH	A	N ₃ -Val ^{uα} -OSu	19
Boc-(L)-Lys(Alloc)-OH	A	N ₃ -Lys(Alloc) ^{uα} -OSu	37
Fmoc-(L)-Trp(Boc)-OH	B	N ₃ -Trp(Boc) ^{uα} -OSu	21
Fmoc-(L)-Arg(Pbf)-OH	B	N ₃ -Arg(Pbf) ^{uα} -OSu	11
Fmoc-(D)-Lys(Boc)-OH	B	N ₃ -Lys(Boc) ^{uα-D} -OSu	33

945 ^aSee **Figure 5**. ^bThe yield corresponds to the overall yield.